ANALYSIS OF MEG SIGNALS FOR SELECTIVE ARITHMETIC TASKS

A dissertation submitted to the Faculty of Engineering and the Built Environment, University of Witwatersrand for the degree of Master of Science in Engineering.

Graham Peyton

April 2014

I declare that this dissertation is my own, unaided work, unless otherwise acknowledged. It is being submitted for the degree of Master of Science of Engineering at the University of Witwatersrand, Johannesburg. It has not been submitted before for any degree or examination at any other university.

Graham Peyton

Signed on: 22 day of April 2014

Abstract

A magnetoencephalogram (MEG) is a non-invasive tool for measuring neuronal activity with millisecond temporal resolution. In this study, MEG measurements were recorded as a subject carried out a simple, repetitive, numerical task: deciding whether a number is even or odd. Signal processing techniques were applied to the MEG data so as to characterise the spatial and temporal dynamics of the brain during the decision-making process. The data is first preprocessed using Independent Component Analysis (ICA) and other semi-automated methods. The data is then segmented into trials. Evoked fields or event-related fields (ERFs), the classical measure of brain activity, are found by averaging all the trials in the time domain. These responses are typically phase locked to the stimulus. Induced potentials or oscillatory rhythms that are not necessarily phase-locked to the stimulus are found by averaging the time-frequency representations (TFRs) over all the trials. The TFRs were found using the Wavelet Transform.

The results show that typical ERF components are present just after the onset of each stimulus. These waveforms indicate that the following sequence of cognitive events occur: mental matching of the stimulus with previously experienced stimuli (N100); higher-order perceptual processing modulated by attention (P200); and "Go-NoGo" control procedure which initiates or inhibits the motor response (N200). The P200 response also indicates that parity information may be retrieved directly from memory rather than being extracted by means of a mental calculation strategy. Time-frequency plots of the data show pronounced synchronisation in the beta-band as the subject is actively concentrating on the mental task. Thereafter, beta band desynchronisation occurs as the motor response is carried out. Activity is pronounced in the left general interpretive area with a latency of around $650\,ms$. This confirms the fact that the brain is lateralised according to function.

One important avenue for further research would be to explore source reconstruction using beamforming techniques. This would enable researchers to pinpoint neuronal sources with greater accuracy. Furthermore, functional connectivity analysis may be a useful means of elucidating how information is transmitted and integrated across brain networks. Overall, there is much scope for future work.

Acknowledgement

I would like to express gratitude to my supervisors, Prof. David Rubin and Adam Pantanowitz for their continual assistance, guidance and support during the course of my Masters research. Thank you for making the research possible and for enabling me to fulfill my dreams! The brain has always been a great interest of mine, and this project has only increased my fascination with it. I would like to thank the University of the Witwatersrand, Johannesburg, for supporting the research financially. Many thanks also goes to Bar Ilan University for providing the project and the MEG data. In particular, I would like to acknowledge Prof. Mina Teicher and Amir Kleks for their willingness to collaborate with us. I would also like to thank my parents, Derek and Kathy, for their unconditional love and support, and my fiancé, Megan, for spurring me on to complete this project. Lastly, and most importantly, I render thanks and praise to God, the Creator of the complexities of the human brain; His wisdom is inscrutable.

Contents

List of Tables

List of Figures

Chapter 1

Introduction

The human brain is arguably the most complex organ in the body, and we know little about its structural and functional complexities. It contains tens of billions of neurons organised into hundreds of neuronal pools that carry out a bewildering number of functions [6]. Over the last few decades, significant effort has been put into understanding how the brain carries out complex cognitive tasks. Magnetoencephalography (MEG) is an excellent tool for measuring the activity of the brain so as to understand its spatiotemporal dynamics. MEG devices measure the magnetic fields produced by the brain using an array of superconducting interface devices (SQUIDs). The SQUID sensors are capable of measuring fields as low as $10fT$ [3].

In this study, subjects were monitored by an MEG device while being shown a series of three digit numbers. The subjects were asked to determine whether the numbers were even or odd, and to push a button to indicate their choice. The objective of the study is to use signal processing techniques to characterise the spatial and temporal dynamics of the magnetoencephalogram (MEG) during a cognitive decision-making process, and so gain a deeper understanding of the aspects of brain function.

The temporal resolution of MEG is in the order of milliseconds; much higher than fMRI and PET [3]. Standard analysis of MEG data involves the use of stimulus-locked averaging over epochs of time to produce an evoked response [3, 7, 8]. During complex cognitive tasks, evoked responses are generated throughout the cortex. Amplitude fluctuations in

these responses is indicative of underlying brain activity. For example, a negative deflection around 100 ms (N100) is indicative of mental matching of the stimulus with previously experienced stimuli [9]. Recently there has also been a great deal of interest in analysis of the so-called "induced response", which corresponds to stimulus-related variations in power in different frequency bands as a function of time [3]. These oscillations themselves are not phase-locked to the stimulus or response [10]. Induced responses are typically analysed using a time-frequency decomposition such as the Morlet wavelet transform. Averaging over epochs of the power in the time-frequency maps gives one an estimate of induced components, which can then be tested for experimental effects [3, 11, 12]. These two forms of processing, stimulus-locked averaging and averaging of time-frequency power maps, are the two basic approaches used in this study for analysing evoked and induced components respectively in the MEG data.

Chapter 2 of this dissertation begins by introducing background concepts relating to the brain and magnetoencephalography. Evoked and induced responses are also discussed together with the signal processing techniques that are used in the analysis. The purpose and rationale of the study are presented in chapter 3. Chapter 4 continues with a detailed discussion of the specifics relating to the computational algorithms. This section also addresses the data acquisition, preprocessing and analysis procedures, and the computational tools used to carry out these procedures. Finally, the results of the analysis are presented in chapter 5, followed by a discussion of the results in chapter 6.

Chapter 2

Background

2.1 Physiological Basis for MEG signals

2.1.1 The Brain

A thorough understanding of the anatomical and functional areas of the brain is critical to properly interpret MEG results. The human brain is divided into the cerebrum, diencephalon (thalamus and hypothalamus), cerebellum and brain stem (mesencephalon, pons, and medulla oblongata) [6]. The cerebrum can be divided into two large, paired cerebral hemispheres. The surface of the hemispheres is covered by a superficial layer of grey matter, the cerebral cortex, which is folded into ridges (gyri) and grooves (sulci) that increase the surface area. Roughly one tenth of all neurons are found in the cerebral cortex. The main focus of MEG studies is the cerebral cortex because of its functional role in cognitive processes and because, as it is the most superficial layer of the cerebrum, it is in close proximity to the MEG sensors [3].

The cerebrum is divided into four topographical regions, as shown in figure 2.1. On each hemisphere, the central sulcus, a deep groove, divides the anterior frontal lobe from the posterior parietal lobe [1, 6]. The lateral sulcus separates the frontal lobe from the temporal lobe. Posteriorly, the parieto-occipital sulcus separates the parietal and occiptal lobes. The two cerebral hemispheres are separated by the longitudinal fissure. Each hemisphere is connected by a band of white matter called the corpus callosum [1, 6].

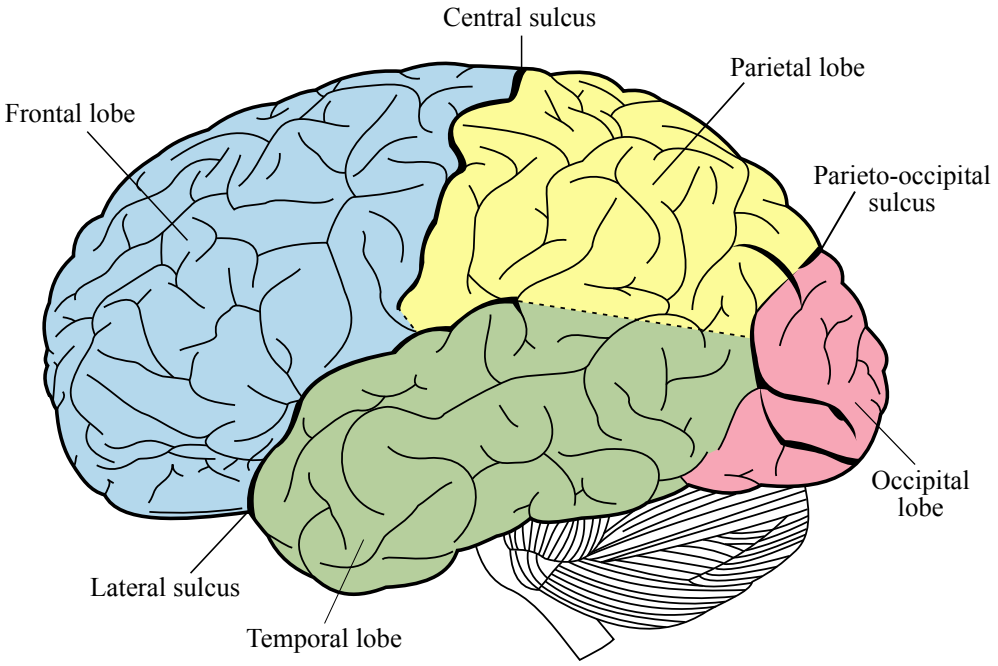

Figure 2.1: Lobes of the left cerebral hemisphere (public domain image adapted from [1]).

The cerebrum is the seat of most higher mental functions, including conscious thoughts, sensations, intellect, memory and complex movements [6]. The visual cortex, located posteriorly in the occipital lobe, is involved in the conscious perception of visual stimuli [13]. The primary motor cortex is located anterior to the central sulcus, while the primary sensory cortex is located posterior to it. These areas are responsible for the control of skeletal muscles, and the perception of somatic-sensory information such as touch or pressure [6, 13].

The sensory and motor areas are connected to nearby *association areas*, which interpret incoming data or coordinate responses. The visual association area, located in the occipital lobe, anterior to the visual cortex, monitors and interprets visual input. The premotor cortex, located in the frontal lobe, anterior to the primary motor cortex, coordinates learned movements [6].

Integrative centres are areas that receive information from the association areas and direct complex motor activities. For example, the prefrontal cortex of the frontal lobe has been implicated in planning complex cognitive behaviour and in decision making. The

general interpretive area (Wernicke's area) is associated with speech, language and mathematical computation [6, 13]. This area is present in the left (dominant) hemisphere only and is located at the border of the temporal, occipital, and parietal lobes. This is an example of hemispherical lateralisation, where different hemispheres are responsible for different functions. Typically, the left hemisphere is important for performing analytical tasks such as calculations or logical decision making. The right hemisphere is responsible for analysing sensory information and relating the body to the sensory environment [6].

2.1.2 Neuronal Currents and External Magnetic Fields

Neurons form the basic building blocks of the nervous system. Neurons are electrically excitable and transmit information through electrical and chemical signals. When activated, they generate time-varying transmembrane electrical currents, as shown in figure 2.2. Rapid depolarisation of the neuronal membrane mediated by voltage-gated ion channels embedded in the membrane results in an *action potential* (AP). The AP propagates as a wave along the axon of the neuron. Each axon connects to the dendrites of other neurons by a connecting junction called a synapse. Chemical neurotransmitters are released into the synaptic cleft; these initiate an electrical response or a secondary messenger pathway that either excites or inhibits the postsynaptic neuron [2, 6].

The neuronal currents generate electromagnetic fields that can be measured using imaging modalities such as EEG or MEG. As mentioned above, there are two sources of neuronal activation: action potentials and post-synaptic potentials (PSP) [3]. MEG is used to measure PSPs because of three factors:

- *Field Decay*. Intracellular currents flow in two directions from the site of the action potential. The resultant quadrupolar field decays as $1/R^3$, where R is the distance from the site. In the case of the PSP, current flows in only one direction, so the source of the field may be viewed as a dipole. The field therefore decays as $1/R^2$, so it persists at distances further away from the source than the quadrupolar field [2].

- *Spatial summation*. Pyramidal neurons of the cortex give the main contribution to MEG measurements since they are arranged in parallel with the apical dendrites aligned perpendicular to the cortical surface. When several neurons in the same

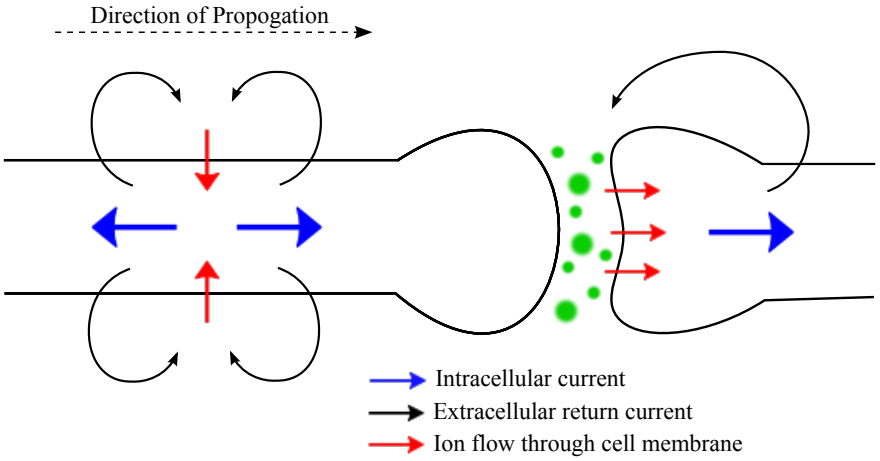

Figure 2.2: Illustration showing neuronal currents: action potential in presynaptic neuron and postsynaptic current induced by synaptic activation (adapted from [2]).

vicinity receive a signal, the PSPs sum spatially, resulting in a stronger field measurable by MEG [2, 3].

- *Temporal summation*. The duration of an AP is approximately $1\,ms$, whereas that of a PSP is approximately $10\,ms$. Typically, it takes several thousand synchronised, spatially-close PSPs to generate a magnetic field strong enough to be detected outside the head. Because the duration of APs is shorter, they would have to be extremely well synchronised to have a marked effect [3].

Because the cortex of the brain is folded, some populations of neurons have apical dendrites that are arranged perpendicular to the skull, i.e., those at the top of the gyrus. Others lie parallel to the skull on the wall of the sulcus [14]. The specific orientation relative to the skull influences the resulting MEG signal recorded outside the skull: MEG only measures fields that have components perpendicular to the device sensors [14]. These fields are generated by neuronal currents that have a component that is tangential to the skull, as shown in figure 2.3.

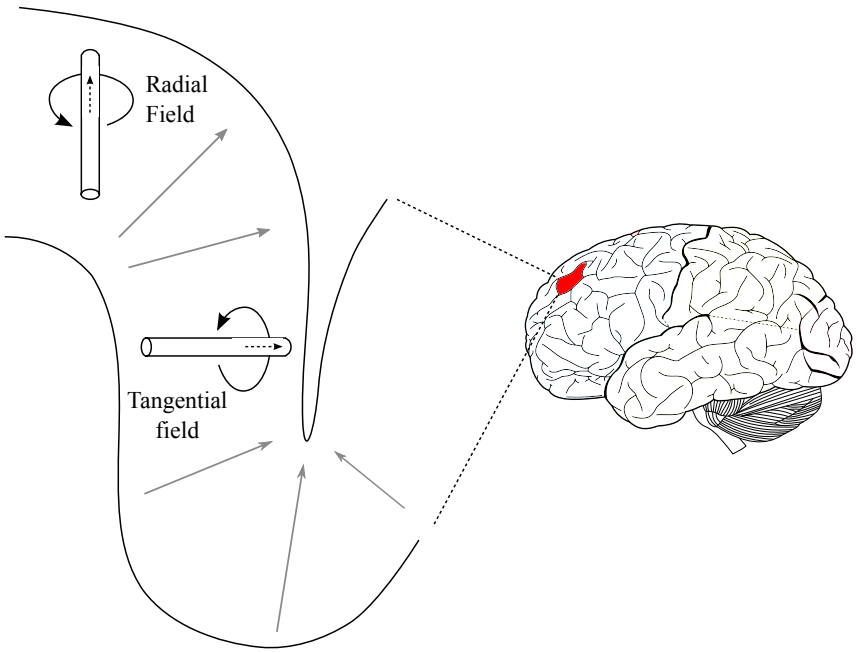

Figure 2.3: Schematic drawing of a piece of cortex showing the crown of a gyrus and a sulcus. Arrows inside the cylinders indicate the direction of PSP flow. Radial and tangential magnetic fields are indicated by arrows (after [1–3]).

2.2 Magnetoencephalography

Magnetoencephalography (MEG) is a technique for measuring the magnetic fields generated by brain activity. MEG signals recorded at the scalp are generated by the synchronous activity of tens of thousands of neurons in the cerebral cortex [3]. Neuronal currents induce weak magnetic fields in the order of femtoteslas which can be measured by an array of very sensitive magnetometers. The only sensor that provides sufficient sensitivity for practical MEG work is the Superconducting Quantum Interference Device (SQUID). A SQUID is an ultra-low noise detector which uses a superconducting ring to measure the magnetic flux and convert it into a voltage [3, 15].

SQUIDs require cryogenic temperatures for operation because they rely on quantum mechanical phenomena found in superconductors. A modern MEG device has an array of often more than 300 SQUIDS mounted in a vessel containing liquid helium. The sensors

allow for simultaneous measurements over the entire cortex. The MEG system is operated in a shielded room that minimises interference from external magnetic disturbances such as the earth's magnetic field, noise generated by electrical equipment and low frequency magnetic field noise sources like elevators, cars, and trains [3].

MEG is different from other modalities such as fMRI, PET and SPECT in that it is a direct measure of brain function instead of secondary measures reflecting brain metabolism. The great strength of MEG (and EEG) is that it provides a very high temporal resolution in the order of milliseconds [15]. Because magnetic fields are less distorted than electric fields by the skull and scalp, MEG provides a better spatial resolution than EEG [3]. However, whereas scalp EEG is sensitive to both tangential and radial components of a current source in a spherical volume conductor (see figure 2.3), MEG detects only its tangential components. In practice, however, this feature is a great asset in source localisation, since it greatly simplifies the "inverse problem" associated with the reconstruction of intracranial neuronal current sources [3].

MEG is primarily used in research as a non-invasive means of measuring the time course of activity in the brain. It has been used to study cognitive processes such as vision, audition and language processing in foetuses and in adults [11, 12, 16]. Other studies have reported successful classification of diseases such as Alzheimer's [17], indicating that MEG may also be used as a diagnostic tool. MEG has also been used in clinical practice to map areas of the brain involved in language performance in order to assist surgery [18].

2.2.1 Dynamic Range and Artifacts

The dynamic range of MEG signals is highly variable between individuals. It is usually a few femtoteslas or picoteslas. Factors that affect the dynamic range are the extent of the activated area, level of neuronal activity, anatomical location and orientation of the neuronal sources, and the amount of destructive interference due to nearby activations. MEG signals are usually several orders of magnitude smaller than unwanted artifacts, which makes artifact removal an essential part of MEG signal preprocessing [3]. Artifacts are unwanted components of data that contaminate the signals of interest. They can be classified into three categories [19]:

1. System related artifacts which are due to electronic SQUID jumps or noisy, broken or saturated sensors.

2. External artifacts, arising from generators of magnetic fields outside the human body such as power lines and other environmental noise sources (elevators, air conditioners, nearby traffic, mechanical vibrations transmitted to the shielded room, etc.).

3. Physiological artifacts caused by eye movements, eye blinks, cardiac and muscular activity, and head movements. The movement of magnetic objects or particles attached or implanted to the body may give rise to artifacts (e.g. eye make-up, hair spray, magnetised dental fillings).

Methods for eliminating these undesirable signals are discussed in section 2.3.

2.2.2 Evoked and Induced Responses

The classical measure of task-related brain activity is the evoked response that is phase-locked to a stimulus [20]. Evoked responses are a subclass of event-related fields (ERFs). ERFs are manifestations of information processing activities, and different types of ERF waveform components are associated with different functions in this process [21]. Studies have shown that in simple motor or sensory tasks, evoked responses arise from the motor or sensory areas of the brain [3]. During more complex cognitive tasks, evoked responses are generated throughout the cortex. For example, an EEG study demonstrated that when a subject carried out a series of selective tasks (differentiating between a real/non-real word or an acute/obtuse angle), an evoked potential occurred in the frontal and parietal regions $160\,ms$ after the onset of the stimulus [22]. Researchers have also used MEG to show that during arithmetic tasks, neural activity occurs in the frontal and pre-frontal regions with latencies of around $700-900\,ms$ [23]. To test for an evoked response, the subject must carry out a task multiple times. The MEG data are averaged over these trials so as to estimate the underlying neural activity [3, 11]. Evoked responses are typically rapidly transient, lasting for less than one second [24].

The brain also produces synchronous oscillatory activity (an induced response) that is not necessarily phase-locked to the stimulus [20]. These rhythms manifest as time-dependant variations of amplitude oscillations within a frequency band of interest [3]. They typically last over a period of several seconds. This extended temporal scale suggests that induced responses are useful in processing sequential events by keeping information available over longer periods of time [24]. Table 2.1 compares the frequencies bands, locations and mental states associated with various types of oscillatory rhythms.

2.3 Signal Processing Methods for MEG

The brain is a complex, dynamic system, so multichannel measurements are necessary to gain an understanding of its behaviour. There are three problems associated with the analysis of multivariate time series [10]:

1. Preprocessing is necessary to remove nuisance components from the data (such as those mentioned in section 2.2).

2. The data must be appropriately represented for the purposes of analysis and visualisation.

3. The underlying features of the signals must be extracted, mostly in the absence of strong models for the dynamics of the relevant parts of the brain.

With increasingly powerful computational resources, it is possible to carry out these steps in a semi-automated way. Parts of the analysis must be automated because the large dimensionality of the data effectively precludes exhaustive manual inspection of the data by the human experimenter. It is important to choose appropriate analytical and computational tools for the analysis. Superficial application of complex signal processing or statistical techniques can lead to erroneous results or conclusions [3]. The techniques chosen for this analysis are discussed below.

Table 2.1: Rhythmic activity in different frequency bands.

Band	Frequency (Hz)	Location	Normal Mental State
Delta (δ)	≤ 4	Broad or diffuse; may be bilateral or widespread.	Drowsiness; lack of attention; sleep [25].
Theta (ϑ)	$4-8$	Regional; may involve many lobes; can be lateralised or diffuse.	Drowsiness; creativity and intuition in adults [6, 25].
Alpha (α)	$8-12$	Regional; usually involves entire lobe; strong occipital with eyes closed.	Relaxing; meditation; closing eyes [26].
Beta (β)	$12-15$ (low-β)	Symmetrical distribution, most evident frontally; localised.	Relaxed and focused. Low-β decreases with motor action; physical restraint increases low-β activity [20].
	$15-18$ (mid-β)		Alert, thinking, aware of self & surroundings [26].
	$18-30$ (high-β)		Alertness; intense, active concentration; mental activity, e.g. math, planning [6, 20, 26].
Gamma (γ)	$30-100$	Somatosensory cortex.	Cross-modal sensory processing (e.g. sight and sound), short-term memory matching, high-level integrated thinking/information processing [12].
Mu (μ)	$8-13$	Sensorimotor cortex.	Mu suppression when performing a motor action [26].

2.3.1 Artifact Removal

There are two general strategies for dealing with artifacts. First, one may identify data segments contaminated by artifacts through visual inspection, by means of an automatic detection procedure, or a combination thereof. The contaminated data segments are excluded from further analysis [19]. The second strategy involves the use of signal processing techniques to reduce artifact components that are not caused by brain activity while preserving signals originating from the brain. These methods often make use of linear transformations or regression techniques applied to the sensor data [19]. For example, linear transformations can be obtained from Principal Component Analysis (PCA), Independent Component Analysis (ICA), Signal Space Projection (SSP) or Signal Space Separation (SSS). The applicability of these techniques relies on the assumption that the spatial topographies of the artifacts are stable across time, and that these spatial signatures can be described with a limited number of spatial components [19].

Independent Component Analysis

Independent component analysis is a multivariate statistical technique which aims at finding linear projections of the data that maximises their mutual independence. In MEG, it is frequently used for the identification and extraction of unwanted artifacts. The data are no longer represented at the level of recorded (scalp) channels, but as a set of virtual channels or components. Certain artifacts are often reflected by a few components which may be identified and then removed. The remaining components can be projected back to the sensor level [3].

In ICA, the data are represented by a random vector $\mathbf{x}(k) = [x_1(k), x_2(k), ..., x_m(k)]^T$, where m is the number of variables (channels) and k the number of observations. For the noiseless case, the observed data is transformed using the following linear transformation [27]:

$$\mathbf{x}(k) = \sum_{i=1}^{m} a_i s_i(k) = \mathbf{A}\mathbf{s}(k)$$

where $\mathbf{A}$ is the mixing matrix composed of constant elements $a_{i,j}$. The source signals or components in the random vector $\mathbf{s}(k) = [s_1(k), s_2(k), ..., s_m(k)]^T$ are stationary, statistically

independent and are non-Gaussian. ICA techniques are used to solve for the mixing matrix, **A**, from which the independent components, $\mathbf{s}(k)$, can be obtained through the matrix inversion:

$$\mathbf{s}(k) = \mathbf{A}^{-1}\mathbf{x}(k)$$

The determination of the independent components begins by centering the data (removing the mean values of the variables) and then whitening or decorrelating the data [27]. The mixing matrix is found by applying a linear transformation to the whitened data. There are numerous approaches for estimating **A**, but they all make use of an *objective function* that is related to variable independence. The function is maximised or minimised by an optimisation algorithm [28]. Implementing the entire ICA algorithm is a nontrivial task. In this analysis, an existing ICA method based on Bell Sejnowski's Logistic Infomax algorithm [29] was applied. The details of this algorithm are beyond the scope of this dissertation.

2.3.2 Spectral Analysis

Rhythmic or oscillatory activity is rarely phase-locked to a stimulus or event [3, 20]. For this reason, averaging cancels out these fields and a different analysis method is required. Oscillatory neuromagnetic signals are typically analysed by examining the spectra of the MEG signals, which are inherently non-stationary [10]. Averaging over epochs in time-frequency maps gives one an estimate of induced components which can then be tested for experimental effects. Methods that are commonly used for spectral analysis are the Fourier Transform, Wavelet Transform, and Hilbert Transform [10, 19]. The choice of the specific spectral analysis method is less critical than its application. In fact, it has been shown that all three methods yield equivalent results in their application to neuronal signals [30].

For this experiment, the Wavelet Transform (WT) is chosen. The Continuous Wavelet Transform (CWT) of a continuous function $x(t)$ is written as [28]:

$$W(a,b) = \int_{-\infty}^{\infty} x(t)\frac{1}{\sqrt{|a|}}\Psi * (\frac{t-b}{a})dt$$

where Ψ is a continuous function in both the time and frequency domains called the mother wavelet, a is the scale factor and b is the translation factor. The factor $\sqrt{|a|}$ is for energy normalisation across the different scales. A popular wavelet, the Morlet Wavelet, is defined by:

$$\Psi(t) = e^{-t^2} cos(\pi\sqrt{\frac{2}{ln2}}t)$$

Intuitively, the wavelet coefficients describe the correlation between the waveform and the wavelet at various translations and scales. One significant problem with the CWT is redundancy which is caused by oversampling the original waveform. This problem is addressed by the Discrete Wavelet Transform (DWT), which is often written in terms of its inverse transform:

$$x(t) = \sum_{k=-\infty}^{\infty} \sum_{l=-\infty}^{\infty} d(k,l) 2^{-k/2} \Psi(2^{-kt} - l)$$

where k is related to a as $a = 2^k$; b is related to l as $b = 2^{kl}$; $d(k,l)$ is a sampling of $W(a,b)$ at discrete point k; and Ψ is the wavelet function [28].

Wavelet analysis is particularly useful in that there is a built-in trade-off between time and frequency resolution. It provides a better frequency resolution (poorer time resolution) when a is large, but better time resolution (poor frequency resolution) when a is small. This makes wavelet analysis useful in analysing non-stationary signals with rapidly varying high-frequency components superimposed on slowly varying low-frequency components [28].

Chapter 3

Aims and Objectives

The objective of this research study is to use computer-based signal processing techniques to characterise the spatial and temporal dynamics of the magnetoencephalogram (MEG) during the cognitive decision-making process - in this case, deciding if a number is even or odd. These characteristics are found by observing evoked responses and synchronous oscillatory rhythms produced in various regions of the brain during the decision-making process.

As this study is an engineering study, the primary objective is the development of suitable computational approaches to analyse the data. The secondary objective is to provide some insight into MEG aspects of the cognitive process, and thereby gain a deeper understanding of how the brain works.

Research Questions

The following research questions must be answered:

- What are the most effective methods and tools for analysing MEG signals? Specifically, what preprocessing and analysis algorithms may be used, and how can the results be visualised? Can current approaches be improved?

- Is an evoked response elicited during each trial period? If so, over what duration does it last, and what frequencies are present? Can event-related field components such

as N100 or P200 be observed, and what does this reveal about the functioning of the brain?

- Can synchronous oscillatory rhythms be observed during each trial period? If so, over what duration do they last, and what frequencies are present?
- Which regions of the brain are most active during selective arithmetic operations? Does this confirm other research findings?

Assumptions

The following assumptions are made:

- At a certain time after the presentation of the stimulus, the brain will process the stimulus. The brain will process repeated stimuli similarly.
- Electrical activity generated by the neurons in the brain has certain properties that distinguish it from artifacts, such as amplitude or distribution. Background noise is stochastic and independent of the triggering events [3].
- The scalp distribution of the MEG depends on the location of the underlying activity.
- Oscillatory activity and evoked responses are produced by specific functional brain regions [3].

Rationale for the study

Neuroscience, the study of the brain, is one of the most exciting and rapidly advancing areas of modern science. Advances in cognitive neuroscience have helped to unravel puzzles of brain development, function and disease. MEG is a particularly useful tool for analysing the brain because it provides a very high temporal resolution and good spatial resolution. This is of great importance when seeking to understand how the brain carries out rapid operations such as arithmetic calculations, object recognition, executive planning and cognitive decisions. Other techniques such as fMRI and PET do not provide real-time

information of neural involvement and are therefore not ideal to track brain activity related to rapid decision-making [3]. The specific objective of this study is to gain a deeper understanding of the time course of neural organisation associated with number processing. The research output will contribute to the field of quantitative neuroscience.

Chapter 4

MEG Data Analysis

4.1 Data Acquisition

A 4D Magnes WH-3600 MEG device located at Bar Ilan University was used to acquire MEG data. The MEG device comprises 248 radial magnetometers covering the entire cerebral cortex. The sampling frequency is $2.0345\,kHz$. The final MEG data structure contains raw MEG data, acquisition parameters, "trigger" event information, and a list of 3-D coordinates describing the participant's head shape.

4.2 Data Preprocessing

The raw MEG data must first be preprocessed before it can be analysed. Preprocessing refers to reading the data, segmenting it around interesting events such as triggers, and removing unwanted artifacts. There are two approaches to preprocessing MEG data. The first is to read continuous data into memory, apply filters, and subsequently segment it. The second approach is to first segment the data, then read those "interesting" segments into memory and apply filters. The first approach is used, as it eliminates the need to deal with edge effects and zero padding of the trials. The disadvantage, however, is that it is memory intensive. The details of the preprocessing procedures are discussed below.

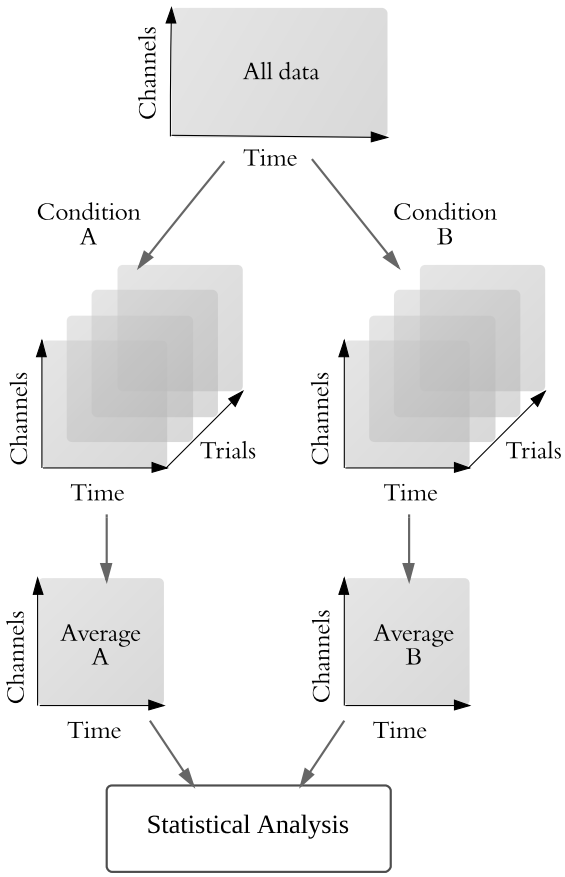

Figure 4.1: Trial-based MEG analysis (after [4])

4.2.1 Trigger-based Trial Selection

A trial-based analysis procedure is used to analyse the MEG data. As figure 4.1 shows, the technique involves segmenting the data with respect to stimulus or condition markers recorded in the data. These segments (trials) are defined by their first and last samples in the dataset. Each trial has an offset that defines where the relative $t = 0$ point (usually the point of the stimulus/trigger) is for that trial. In this analysis, trials begin $0.5\,s$ before the stimulus onset and $1.5\,s$ after the stimulus onset. Only trials where the subject chose the correct answer (even/odd) were considered. Trials and channels contaminated by artifacts were eliminated through visual artifact detection, as discussed below.

4.2.2 Artifact Removal

As stated in section 2.2, artifacts are unwanted components of data that contaminate the signals of interest. These components reduce the accuracy of subsequent analyses. Since artifacts can never be completely eliminated through careful preparation and instruction of participants, it is essential that they are removed using various signal processing methods.

In addition to the techniques discussed below, a script supplied by the Gonda Brain Institute at Bar Ilan University was used to clean the MEG data [31]. The script makes use of environmental magnetic noise from distant magnetic sources using an array of reference sensors mounted in the MEG device. These additional signals are used as regressors for cleaning the main MEG signals using signal processing techniques similar to adaptive filtering. For example, the script eliminates noise due to building vibrations based on accelerometers recording. It also cleans the data based on reference channels by applying different sets of weights for different frequencies. Lastly, it cleans the data of any remaining cardiac or eye blink artifacts or saccades.

Baseline Correction

During the recording, MEG signals often undergo slow shifts in time with respect to the zero level. These shifts may be due to increased background brain activity, muscle activity or other noise sources. A "baseline interval" is defined where one may assume that the brain is not producing any stimulus-related activity. Any shift from the average over this interval is interpreted as a spurious D.C. offset caused by some noise source. In this study, the baseline interval is defined from $-500\,ms$ to $-100\,ms$ relative to the $t = 0\,s$ (stimulus onset) point. This interval is safely within the $1\,s$ pause between the response and the following trigger. For each channel, the mean of this baseline interval is recorded and subtracted from the rest of the signal at all points.

Filtering

MEG responses typically contain frequencies up to about $100\,Hz$ with a roll-off towards higher frequencies. The frequencies of interest are found between $0 - 100\,Hz$ [3]. For this

reason, a fourth order bandpass filter with cutoff frequencies at $1\,Hz$ and $100\,Hz$ has been chosen. The following artifacts are also present in the data:

- $24\,Hz$ noise due to the air conditioning system in the building.
- $50\,Hz$ noise of the electricity system supplied to the MEG.
- Noise due to the building's elevator.

The $24\,Hz$ and $50\,Hz$ noise is eliminated using two notch filters at these frequencies. The elevator's noise is ignored since the elevator movement is erratic and unknown. It should be noted that the filters are applied *before* segmenting into trials - i.e., to continuous data. In this way, one does not have to worry about edge effects and zero padding the trials.

Visual Data Inspection

A common manual artifact detection method involves visually inspecting data and identifying the trials and channels that are affected and should be excluded from the analysis. The visual inspection results in a list of noisy data segments and channels, as shown in tables A.1 - A.2 in Appendix A. An example of noise caused by muscle contractions is shown in figure 4.2. The figure shows the signals for all channels for a single trial period. One can clearly see that high amplitude, high frequency noise has contaminated the trial. Two other examples of noise caused by head movements and electronic SQUID jumps are shown in figures B.1 and B.2 in appendix C.

The number of remaining clean trials for all conditions for all four subjects is larger than the suggested minimum of 60 trials [3]. However, because the number of clean trials for each condition and subject is not identical, the statistical comparison (section 4.3.2) is slightly biased.

After the most obvious artifacts are identified and the contaminated trials removed, the data are also inspected by viewing a plot of the variance for each trial and channel. Trials or channels above a certain variance threshold are eliminated. The variance thresholds for all subjects and conditions are shown in table 4.1. There is no standardised method for choosing the threshold. In this experiment, a threshold was chosen such that a minimum

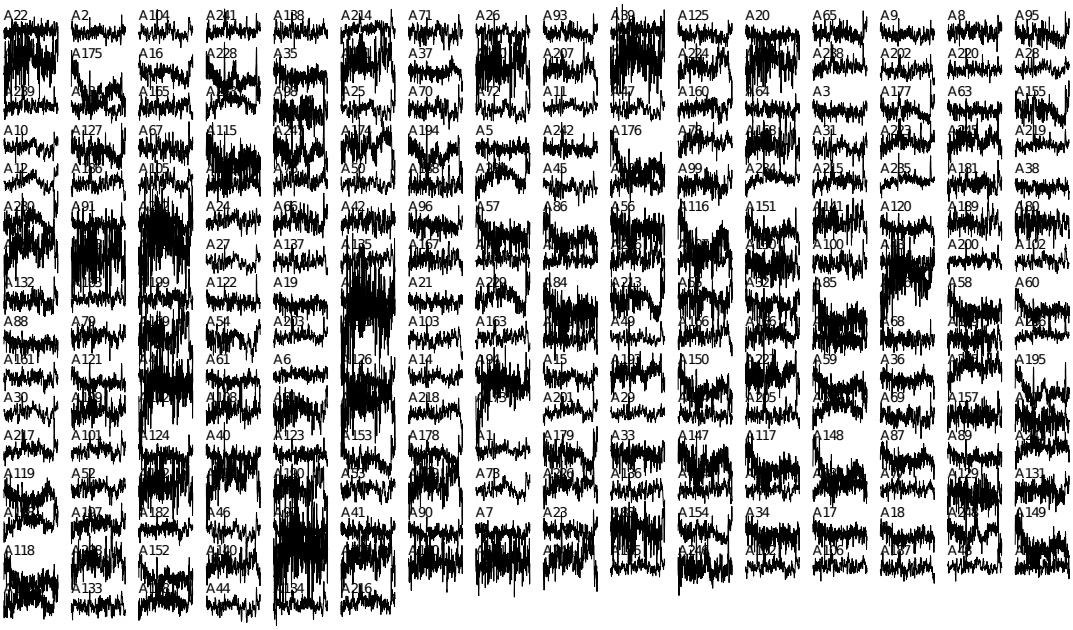

Figure 4.2: Data segment for all channels showing noise caused by muscle contractions.

Table 4.1: Variances for all conditions and subjects.

	Subject 1	Subject 2	Subject 3	Subject 4
Even	3×10^{-25}	4×10^{-25}	5×10^{-25}	3×10^{-25}
Odd	3×10^{-25}	4×10^{-25}	5×10^{-25}	3×10^{-25}
No Number	3×10^{-25}	4×10^{-25}	5×10^{-25}	3×10^{-25}

number of trials were removed (minimum data loss), and a maximum amount of noise was eliminated.

Subtraction of Spatio-Temporal Artifact Contributions

Severe contamination of MEG activity by eye movements, blinks, muscle, heart and line noise is a serious problem for interpretation and analysis. Simply eliminating all contaminated trials results in a considerable loss of information. Other techniques like independent component analysis (ICA), introduced in section 2.3, can eliminate these artifacts without resulting in a significant loss of information. ICA results are generally more favourable

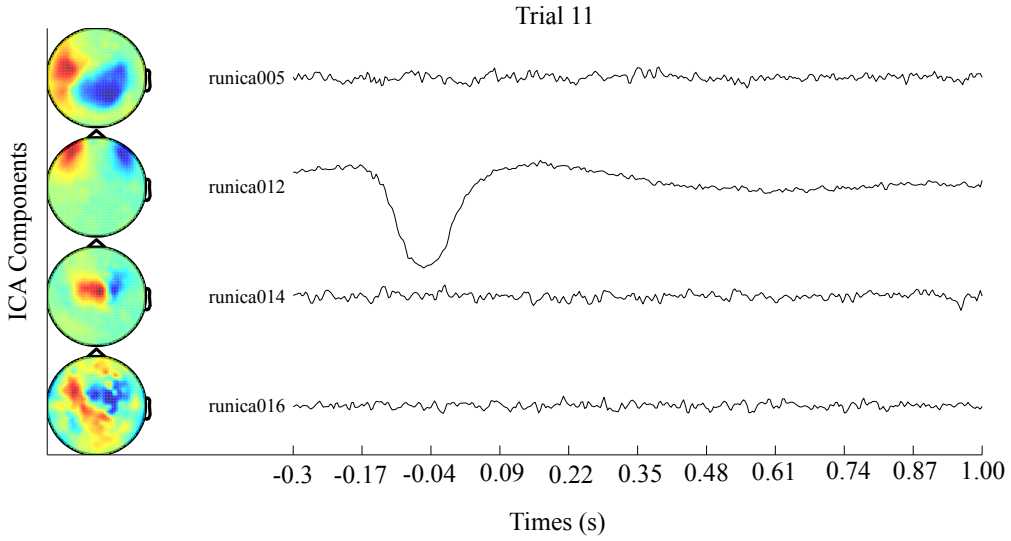

Figure 4.3: ICA components reflecting an eye artifact.

than principle component analysis (PCA) or regression-based methods [32]. ICA is used to represent the data as a set of virtual channels or components that are maximally temporally independent. Certain artifacts, such as those caused by eye blinks or the heart, are often reflected by a few components which are easy to identify visually. These components can then be removed from the data and the remaining components can be recomposed or projected back to the sensor level.

Figure 4.3 shows four ICA components. The second components (runica012) clearly demonstrates an eye blink artifact. This is confirmed by the pronounced ERF activity over the two frontal regions above the eyes. This is probably due to contraction of the extraocular or levator palpebrae superioris muscles. Figure 4.4 also shows four ICA components. The second component (runica006) shows the cardiac artifact. The QRS complex is clearly visible, and there is a period of approximately 0.9 seconds between each pulse, which translates to a heart rate of around 54 beats/min.

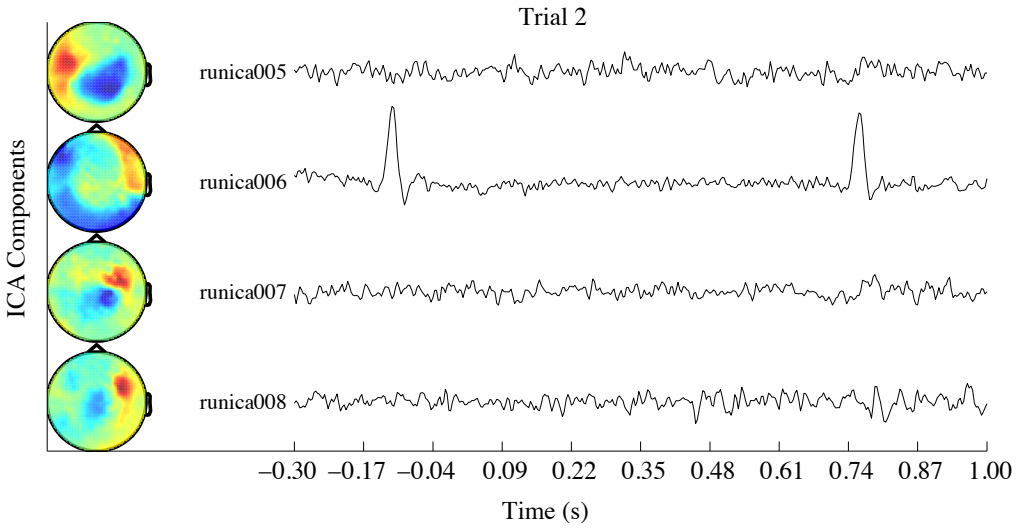

Figure 4.4: ICA components reflecting a cardiac artifact.

4.3 Analysis of Event-Related Fields

4.3.1 Time-locked Averaging of all the Trials

When analysing MEG signals, the aim is to investigate the modulation of the brain with respect to the given event. The assumption is made that the effect of focused mental selection is time-locked to the triggering event (display an even/odd number). Figure 4.5 shows the analysis protocol for analysing event-related fields. Signals from multiple trials are averaged and time locked to the event. This process yields an event-related field (ERF) with a higher signal-to-noise ratio (SNR) [3, 19]. The noise is reduced by a factor of $\frac{1}{\sqrt{N}}$, where N is the number of averaged trials. After averaging, the results are visualised graphically: ERFs for all sensors are plotted topographically according to their position on the MEG helmet. An example of a topographical map is shown in figure 5.1. Individual or spatially averaged ERFs may also be plotted so as to identify interesting signal features.

4.3.2 Statistical Analysis

The objective of a statistical analysis is to determine whether there is a difference in the data for the different conditions (even, odd or no number). A result is statistically significant if

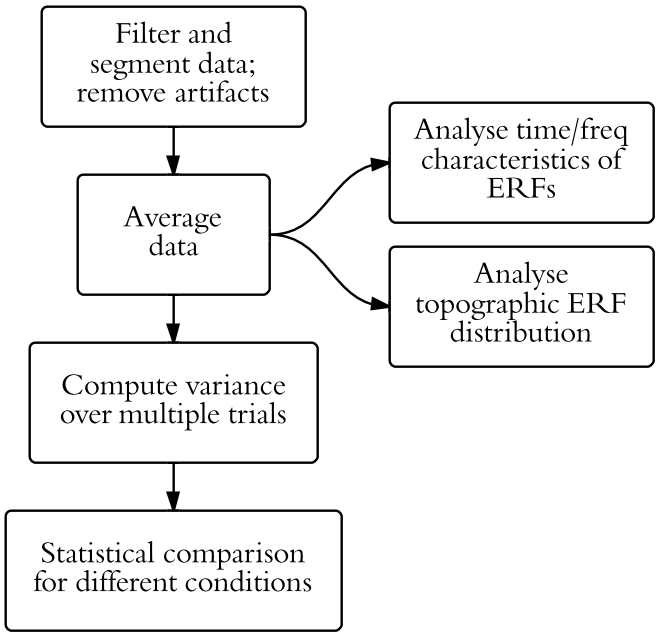

Figure 4.5: Analysis Protocol for Event-Related Fields (ERFs) (after [4]).

it is unlikely to have occurred by chance - i.e., if the probability of its occurrence is greater than some predefined probability threshold, the significance level.

There are two types of statistical methods: descriptive and inferential [33]. A descriptive statistic describes the main features of a dataset. For example, a descriptive statistic may be the maximum magnetic field value within a certain time frame, the average alpha band power of multiple trials, or the latency of beta rhythm onset. Once descriptive statistics have been found for the dataset and a probability distribution assumed, inferential statistics may be used to compare datasets and test hypotheses [33].

In this experiment, a dependent t-test for paired samples is used to test the null hypothesis that there is no statistical difference between pairs of conditions: $H_0 : \mu_1 = \mu_2$ [3], where μ is the mean for a certain condition. This approach has also been used by previous researchers to evaluate the difference between "baseline" and "active" intervals [2]. The assumption has to be made that the data fits a normal distribution, which is reasonable for averaged responses due to the central limit theorem [3]. As equation 4.1 shows, the t-test compares the means of pairs of conditions [33]:

$$t = \frac{\overline{X}_D}{s_D/\sqrt{n}} \tag{4.1}$$

where $\overline{X}_D$ is the average and s_D the standard deviation of the difference between samples, and n is the number of samples. The resultant p-value is compared to the significance level ($\alpha = 5\%$) to test the validity of the hypothesis.

An important feature of MEG data is that it has temporal *and* spatial characteristics. It is fairly trivial to carry out a t-test on a single channel; however, the statistical analysis is complicated by the fact that there are multiple channels. The so-called "multiple comparisons problem" (MCP) arises when one considers a set of statistical inferences simultaneously [34]. The MCP arises out of the fact that the effect of interest (a difference between conditions) is evaluated at an extremely large number of channel/time pairs [3]. Because of the large number of comparisons, it is difficult to control the false alarm or family-wise error rate (FWER) - the probability of falsely concluding that there is a difference between the conditions at one or more channel/time pairs [3]. With an alpha of 5%, there is a 5% chance of rejecting the null-hypothesis. That false alarm rate applies to each test that is performed, so the chance of making a false alarm with 248 subsequent tests is much larger than the desired 5%.

The classic approach to the multiple comparison problem is to control the FWER by applying the Bonferroni correction [34]. Instead of choosing a critical p-value for significance of 0.05, a lower value is used. The significance level (alpha) for an individual test is found by dividing the FWER (0.05) by the number of tests (n). Thus, the new significance level is $0.05/248 = 0.0002$. The disadvantage of this method is that it increases the probability of false negatives; i.e., falsely concluding that there are no differences between conditions.

4.4 Spectral Analysis of Induced Potentials

As mentioned in section 2.3.2, induced oscillatory activity in the brain is rarely phase-locked to the stimulus. Oscillatory activity cannot be observed in event-related fields because averaging cancels out the induced signals [3]. Instead, the event-related changes of

induced activity are analysed by computing and visualising the time-frequency representations (TFRs) of the power. The power spectra for each trial are calculated and finally averaged. To visualise the event-related power changes, normalisation with respect to a baseline level must be performed. There are three ways to graphically present the data [35]:

1. Time-frequency plots of all channels, in a quasi-topographical layout.

2. Time-frequency plot of an individual channel.

3. Topographical 2-D map of the power changes in a specified time-frequency interval.

The spectral analysis is carried out using wavelets. Wavelet analysis is applied to each trial, and time-frequency representations (TRFs) of powers are then averaged across trials [3, 12] in order to visualise the induced fields.

An important consideration impacting the implementation of the wavelet algorithm is the effect of boundary artifacts. The wavelet transform is found by calculating the convolution between the input signal and wavelet function. As the wavelet gets closer to the edge of the signal, the computation requires the presence of non-existent values beyond the boundary [36]. If the resultant boundary effect is not dealt with correctly, it may lead to a considerable loss of information. One may simply accept the loss and truncate unfavourable results at the boundaries. However, crucial frequency information is then lost: one would not be able to ascertain whether low frequency induced potentials are present. Another approach is to extend the boundaries before processing the signals [36]. This could be done artificially or by simply increasing the length of trial on either side of the period of interest. The latter approach was used in this analysis. The disadvantage of extending the boundaries, however, is that it is computationally expensive. In this analysis, the total computation time required to find the TFRs for all subjects and all conditions is approximately 6-7 hours. Overall, however, the result is good - there is only a minimal loss of information at $1\,Hz$ and $2\,Hz$ as shown in figure 5.5 in chapter 5.

4.5 Computational Tools and Techniques

Numerous open source toolboxes are available for MEG analysis. The Gonda Brain Institute at Bar Ilan University provides stable working versions of FieldTrip and the pdf4D

package for reading, writing and analysing 4D-neuroimaging format data files [31]. The FieldTrip toolbox is MATLAB-based, and was used extensively to implement all the analysis procedures described above.

MEG analysis procedures are complex and computationally demanding because data from multiple trials, channels, conditions and subjects must be analysed. A single trial lasting approximately $3\,s$ has approximately 6100 samples. There are around 350 trials per subject. Four subjects were used in the experiment. This translates to a total number of about 8.5 million samples.

Because of this, it was necessary to distribute the computations over multiple processors. Analysis of multiple subjects or conditions is carried out independently on multiple cores. To accomplish this, the MATLAB code was parallelised using the MATLAB Parallel Toolbox. Overall, the total computation time was around six hours when the computations were split over four 2.9 GHz i7 cores. The vast amount of data also introduces memory issues. It is necessary to save the intermediate data of each step to disk, and to load it upon the next (parallel) step in the analysis.

Distributing the code is not the only issue that must be considered when writing MEG algorithms. "Batching" refers to a method of automating and streamlining the algorithm steps into a single protocol which can be repeated over all subjects and/or conditions. The batch algorithm should be executed with a single command and is usually left to run overnight. This method not only increases the efficiency of the algorithm, but it also ensures that the results are reproducible for all subjects and conditions [5]. Figure 4.6 shows an example of a typical analysis pipeline.

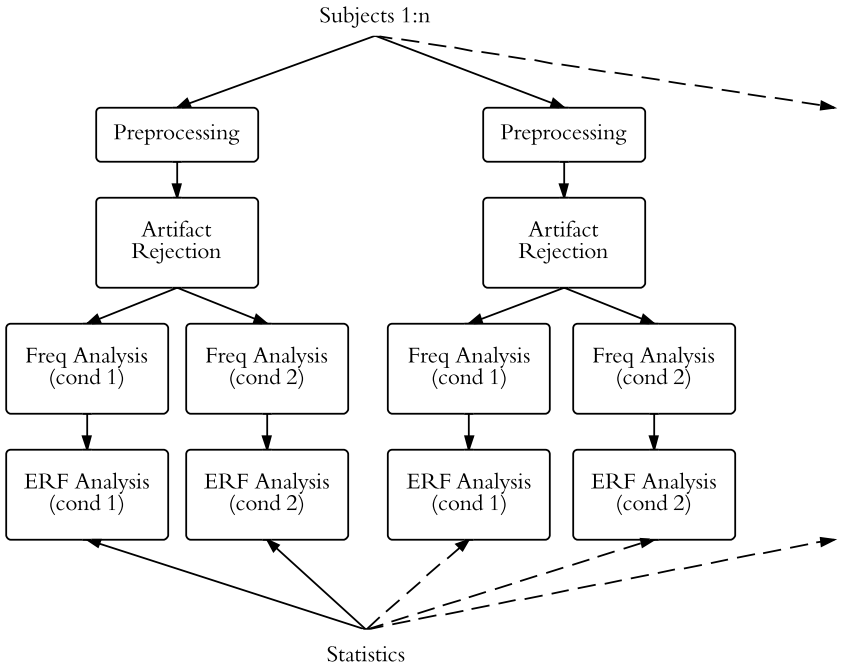

Figure 4.6: Simplified Analysis Pipeline (after [5])

Chapter 5

Results

5.1 Experimental Setup

Two separate MEG recordings ($7-8$ minutes long) were taken using a 4D Magnes WH-3600 MEG device located at the Gonda Brain Research Centre at Bar Ilan University in Israel. The experiment was designed and carried out by researchers at the Gonda Brain Research Centre prior to the start of the present study and without the involvement of the author of this dissertation.

Four anonymous subjects were used in the experiment. All subjects are perceived to have no known pathology. The subjects were seated in a relaxed position in the MEG. Three-digit numbers were displayed one after another. A total of 200 numbers were shown and the subjects had to push one button for an odd number and another for an even number. Each repeating trial therefore includes the following sequence of events:

- Subject sees the number.
- Subject cognitively assesses "even vs odd."
- Subject pushes a button to register the choice.

The numbers were displayed for as long as needed (until a button press). There was a one second break between a button press and the screening of the next number. During this

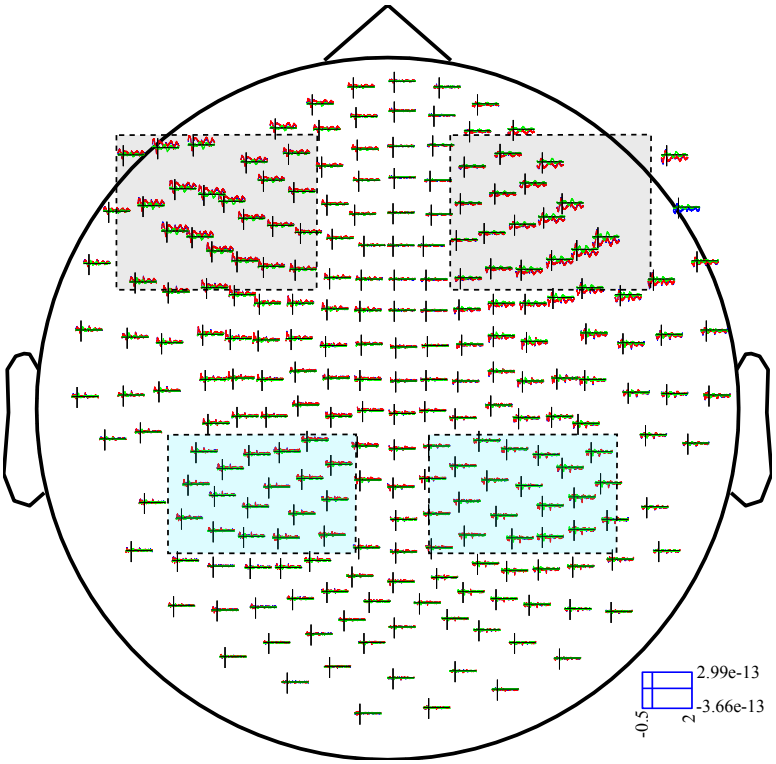

Figure 5.1: ERFs for all conditions over the whole scalp.

break, a small cross was shown to the user to keep their attention. Occasionally, no number is displayed. In this case, the cross is not displayed.

It should be noted that stimulus markers for the “even”, “odd” and “no number” conditions are recorded together with the raw MEG data. The time $t = 0\,s$ corresponds to the onset of a stimulus, as indicated by the appropriate marker. Markers enable one to carry out time-locked analysis of the data.

5.2 Event-related Fields

Figure 5.1 shows a plot of the event related fields (ERFs) for all sensors arranged topographically according to their position in the virtual helmet of the MEG chamber. The ERFs are averaged over all four subjects. By viewing the ERFs in this way, it is easy to identify where significant amplitude variations occur and where differences exist between

conditions. The shaded regions in figure 5.1 show areas where there is a pronounced difference between conditions. Figure 5.2 shows the ERFs for each individual subject.

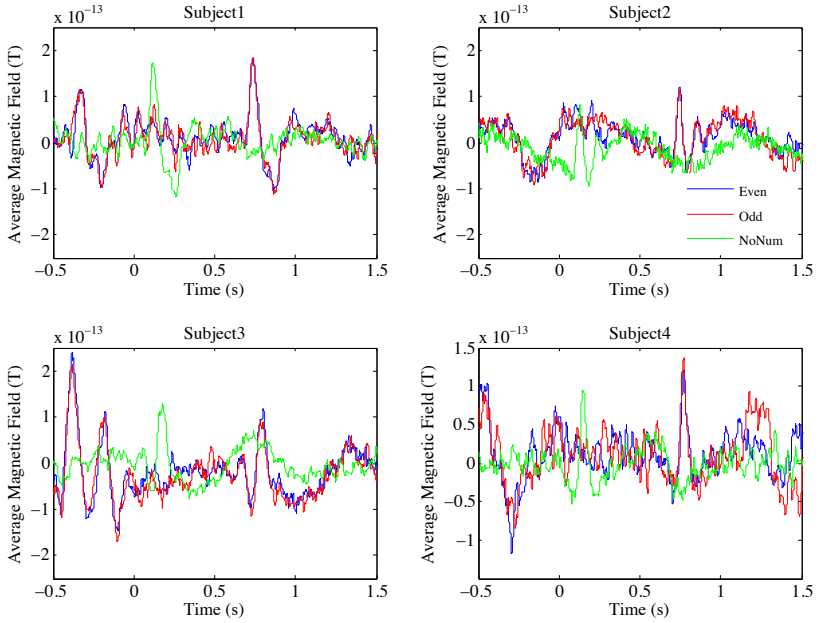

Figure 5.2: ERFs in the left parietal region for all conditions and all four subjects.

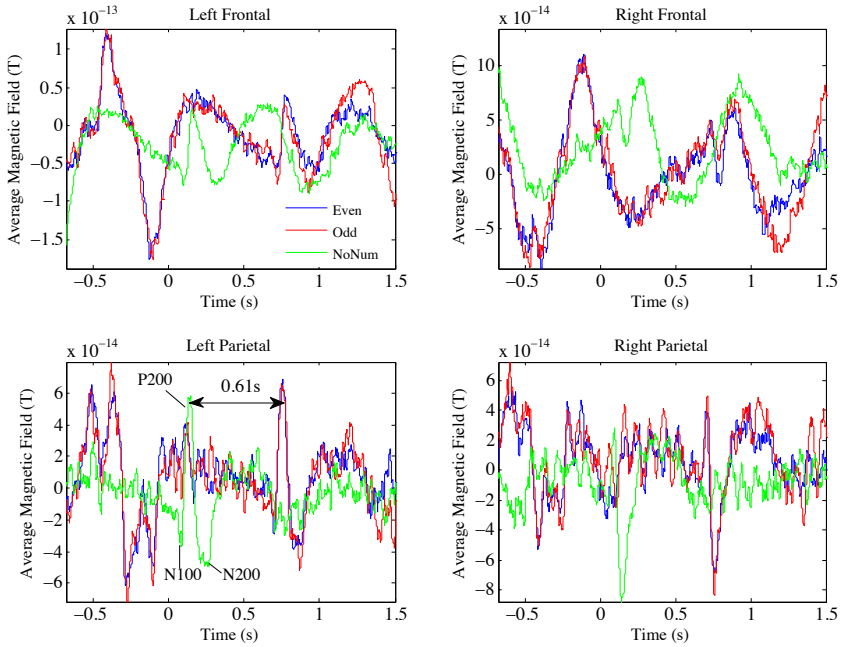

Figure 5.3: ERFs for all conditions averaged over regions of the brain (left/right frontal and left/right parietal).

These signals are averaged over all the ERFs in the left parietal region (i.e., a regional average). There are marked differences between individuals. While certain signal features are common to all subjects, subject 3 demonstrates pronounced oscillatory activity before the onset of the stimulus at $t = 0\,s$.

The averages of all the ERFs in the shaded regions is shown in figure 5.3. The chosen time interval for the trials was from -0.5 s to 1.5 s. The stimulus is presented at $t = 0\,s$. For significant portions of time, signals on opposite hemispheres are inverted in amplitude. It should also be noted that ERFs for "number" (even or odd) and "no number" conditions are similar in shape, but time-shifted by approximately 0.61 s, as indicated in figure 5.3 (left parietal region). Lastly, one can see that significant amplitude variations occur before the onset of the stimulus. This anticipatory response or "readiness field" is discussed in the following chapter.

Typical event-related field components are also present. ERFs are manifestations of information processing activities, and different types of ERF components are associated

with different functions in this process and complimentary brain activity [9, 21]. For example, considering the "no number" condition in figure 5.3 (left frontal and left parietal regions), one may observe negative deflection around $100ms$ (N100 wave), followed by a positive deflection around $200ms$ (P200), and a negative deflection around 200-$350ms$ (N200) [9, 37]. The P200 and N200 waveforms are slightly larger than over the frontal region than over the parietal region. According to current research findings, these waves may be indicative of the following sequential events in the brain:

- Mental matching of the stimulus with previously experienced stimuli (N100) [9]. The N100 depends upon the unpredictability of the stimulus: it is weaker when stimuli are repetitive, and stronger when they are random [38]. In this experiment, the stimuli are repetitive but not completely predictable. This is likely the reason for the small N100 amplitude.

- Higher-order perceptual processing modulated by attention (P200). This wave is typically elicited as part of the normal response to visual stimuli. P200 may be a part of the cognitive matching system that compares sensory inputs with stored memory [39].

- "Go-NoGo" control procedure which initiates the motor response (button press) [37].

It is surprising that these waveforms are elicited at all when no number is displayed; the brain still seems to carry out computational procedures despite there being no number. This phenomenon may be the result of expectation associated with short-term memory - i.e., prior monotonous repetition of a logical operation may lead to the subconscious execution of the same procedures in subsequent trials, even when the procedures are inconsequential.

For the even/odd conditions, similar waveforms appear approximately $610ms$ *later* in time. Because the waveforms are so similar, it is assumed that the same events occur but that they are merely delayed in time. This is not surprising since other research findings show that during arithmetic tasks, neural activity occurs in the frontal and pre-frontal regions with latencies of around 700-$900ms$ [23]. One possible explanation for this is that the presence of an actual number may introduce additional complexities into the computation procedure, thereby slowing down the response.

5.2.1 Statistical Analysis

A statistical test is useful to determine whether there is a significant difference between conditions. A dependent paired samples t-test was carried out on the ERFs shown in figure 5.3 (left parietal region). The difference between the "even" and "no number" trials was evaluated first. The p-value is consistently lower than the significance level (5%) for the entire trial period, except at the following intervals:

- 0.30-0.55 s: $t = -1.574$, $p = 0.116$.
- 1-1.25 s: $t = -0.930$, $p = 0.353$.

During these intervals, there is no statistically significant difference between conditions since the p-value exceeds the 5% level. Visual inspection of the waveforms in figure 5.3 is consistent with this fact. At other time intervals, there is a clear statistical difference between conditions.

The second test evaluated the difference between "even" and "odd" trials. The p-value exceeded the 5% level for almost the entire trial period showing that there is no significant difference between the two conditions. This is also evident in figure 5.3.

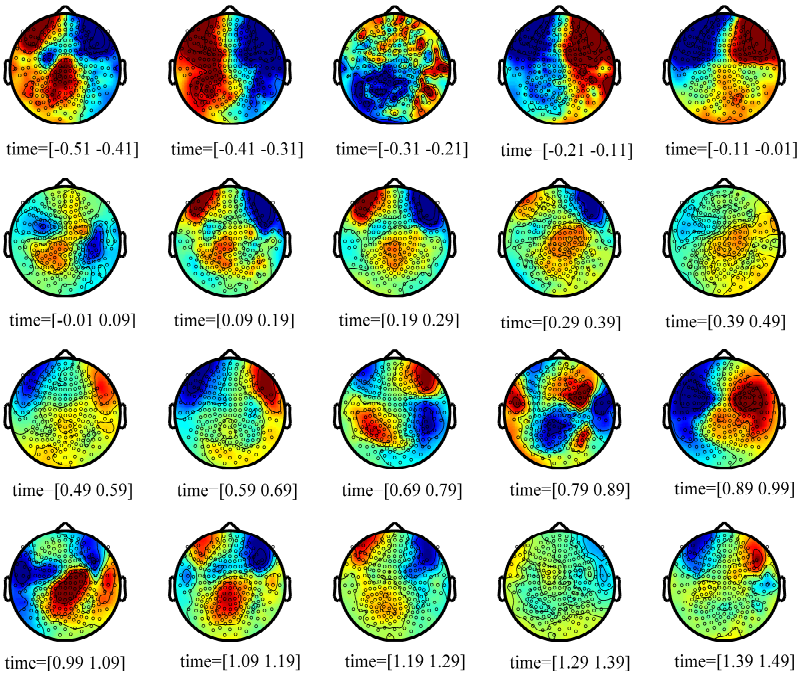

(a) Even condition

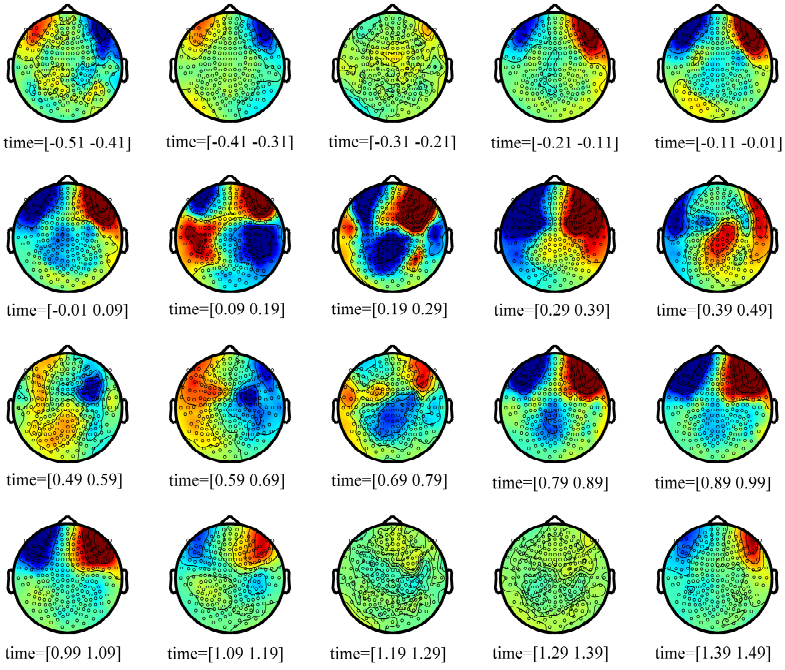

(b) “No number” condition

Figure 5.4: Topographical distribution over the head of ERFs from -0.51s to 1.49s for the even and “no number” conditions.

5.2.2 Topographical Maps of ERFs

A topographical map of the ERFs over the scalp provides useful information about activity in the functional regions of the brain. Figure 5.4a shows a topographical distribution over the head of event related fields from -0.51 s – 1.49 s for the even condition. Observe, firstly, that a clear dipole is present across both hemispheres, particularly in frontal and parietal lobes (-0.41 s to -0.31 s). The dipole then disperses into isolated regions of activity. Immediately prior to the onset of the stimulus (-0.21 s to -0.01 s), the dipole polarity switches. This is assumed to be an anticipatory response. Thereafter, there is a brief increase in ERF amplitude in the left parietal region (P200), and the frontal dipole switches back to its original polarity. The brain continues in this state until 0.7 s, when a second non-symmetrical dipole develops over the general interpretive area (junction of temporal, parietal and frontal lobes). Since this area is involved in logical decision making, the brain is likely involved in carrying out the mathematical operation during this time period. Almost immediately after this (0.79 s to 0.89 s), there is a marked increase in ERF amplitude in the right motor and premotor cortices in the frontal lobe. This indicates that a motor action is occurring (button press) on the contralateral side (left hand).

A topographical map for the "no number" condition is presented in figure 5.4b. The most significant difference is that the frontal dipole polarity does not switch and no parietal dipole persists at the 200 ms (P200).

5.2.3 Power Spectrum of ERFs

Figure 5.5 shows a time-frequency representation of the ERFs averaged over the parietal region. There is a clear correlation between the time-domain signals presented above and the frequency information presented in figure 5.5. In particular, there is an increase in 5-6 Hz activity immediately prior to the stimulus onset (the readiness potential), followed by a suppression thereof. After that, there is an increase in 5-6 Hz and 8-12 Hz activity at 0.7 s, which characterises the delayed P200 wave. It should be noted that this TFR does not provide any information about induced activity (oscillatory rhythms). It represents only the frequency information of evoked fields.

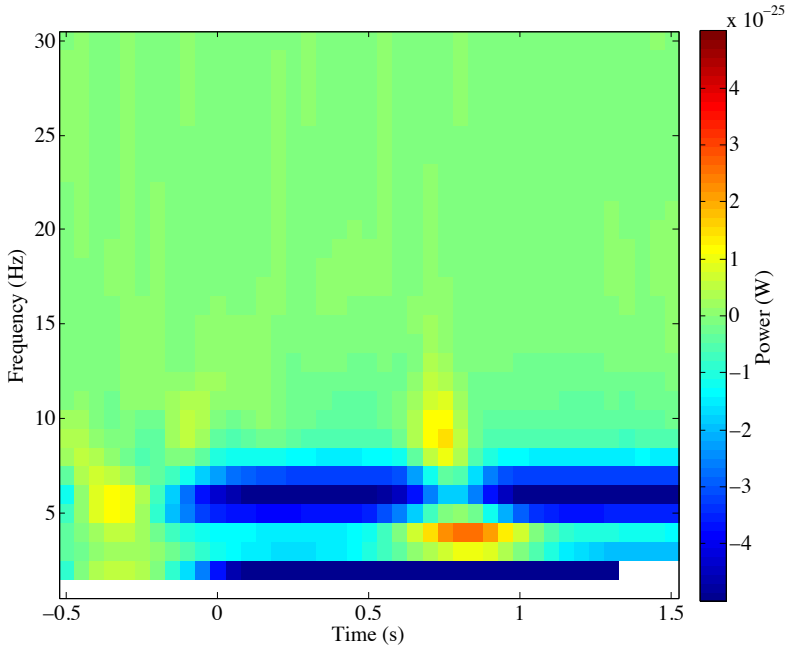

Figure 5.5: Time-frequency representation of ERFs averaged over parietal region.

Boundary effects are present for the lower frequencies (the white time frequency points in figure 5.5). The cause of these boundary effects is discussed in section 4.4. These effects are minimised by increasing the length of the trials beyond the region of interest.

5.3 Induced Fields / Oscillatory Rhythmic Activity

As with the ERF analysis, it is useful to plot the time-frequency representations (TFRs) for all sensors arranged topographically according to their position in the helmet. This is shown in figure 5.6. In this way, one can easily identify induced fields or other interesting effects.

The two bilateral areas of interest are shaded in figure 5.6. Averages of all the TFRs in these regions are shown in figure 5.7 for both the even and “no number” conditions. The TFR for the odd condition is not shown as it is practically identical to that of the even condition.

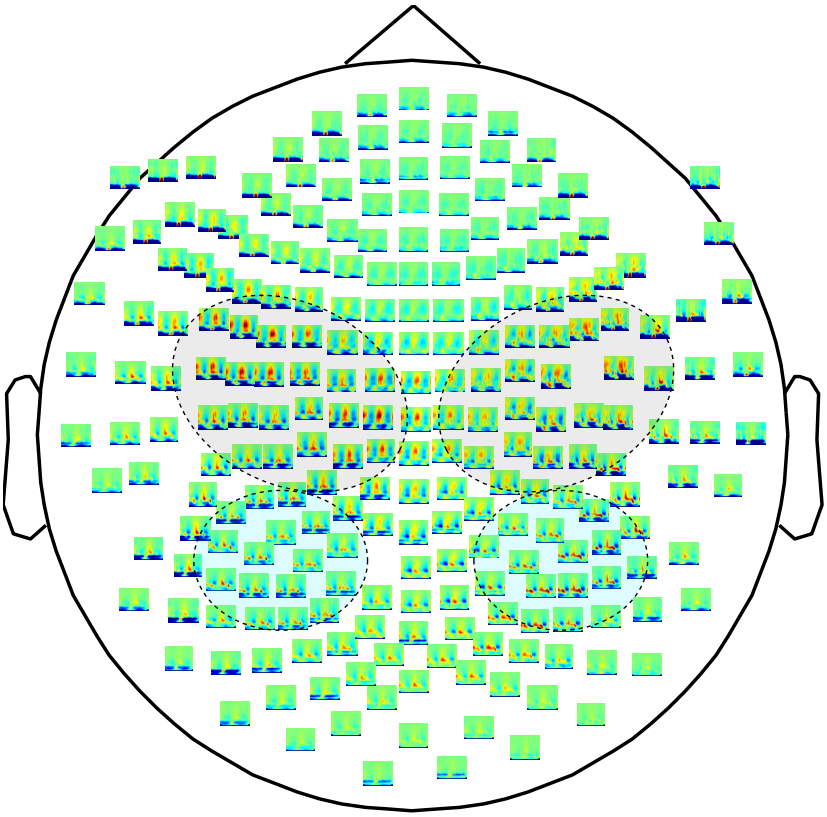

Figure 5.6: Topographical map showing TFRs for all conditions over the whole scalp (even condition).

5.3.1 Even and Odd Conditions

The frontal region (shaded grey) lies over part of the motor and premotor cortices, as shown in figure 5.6. In this region, beta activity (12-30 Hz) occurs from -0.25 s to 0.6 s . From 0.75 s to 1.25 s, the beta activity is suppressed. These two frequency changes correspond to two events. According to table 2.1 in section 2.2, the first event shows that the subject is relaxed, focused, alert and actively concentrating on the mental task. The second event (beta suppression or desynchronisation) is characteristic of a motor response - pressing the button to select even or odd. It is interesting to note that there is a brief increase in delta/theta activity (0-8 Hz) from -0.5 s to -0.4 s which would indicate that the subject is possibly inattentive during the delay between numbers. Thereafter, delta/theta activity is

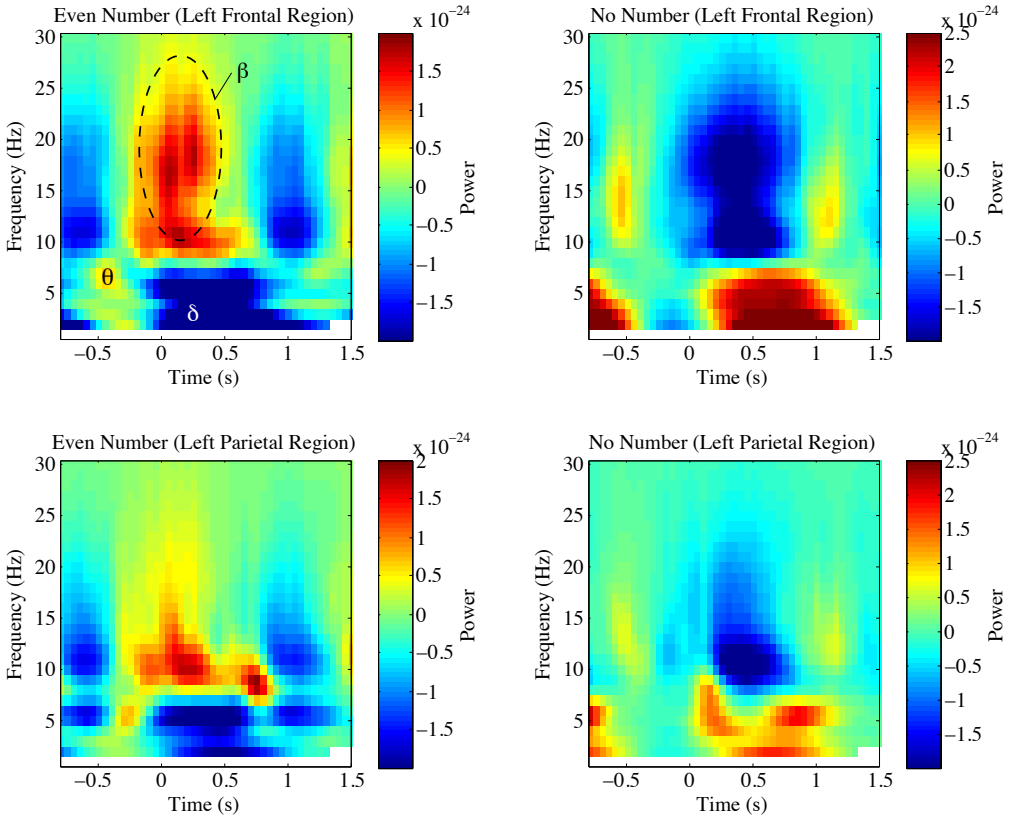

Figure 5.7: TFRs over the frontal and parietal regions for the "even" and "no number" conditions.

dramatically reduced as the subject carries out the cognitive task. The TFRs are limited to 0-30 Hz as no gamma activity is observed above 30 Hz.

Posteriorly, the blue-shaded region shows low-β and mid-β activity over the parietal lobe, close to the general interpretative area. High-β activity is not as apparent as in the frontal region. There is also a similar suppression of beta activity after 0.75 s. Furthermore, there is an identical change in theta activity.

5.3.2 "No Number" Condition

The average TFR in the left frontal region corresponding to the "no number" condition is very different. There is a momentary increase in beta activity followed by a prolonged

suppression of beta activity. This would usually suggest that motor activity is occurring; however, since the subject is inactive during the period, there is likely another reason. One study suggests that beta-band desynchronisation can occur during categorical action planning [40]. The author proposes that the brain subconsciously plans for the next event during periods of idleness (when no number is displayed). Interestingly, however, there is also a marked increase in delta and theta activity during the same period. This would indicate that the subject is possibly inattentive as he/she waits for the next trial.

5.3.3 Topographical Distribution of Beta Activity

The analysis above is further elucidated by the series of topographical maps shown in figure 5.8. This figure shows the time-course of beta activity over the brain. From -0.3 s to 0.4 s beta activity occurs over most of the parietal lobe and part of the frontal lobe. ERF findings in section 5.2 suggest that this activity indicates cognitive activity as the user determines the parity of the number. For 200 ms after this, the beta activity concentrates around the motor cortex (medially) and motor association area (laterally). Activity in the motor association area is indicative of a motor readiness potential (RP) [3]. Since RPs last for several seconds, it may be possible that the RP in this experiment starts earlier (between $0-0.4\,s$) and that during this period it is "masked" by other cognitive activity associated with the mental calculation. Thereafter, the beta activity is suppressed as the subject presses the button.

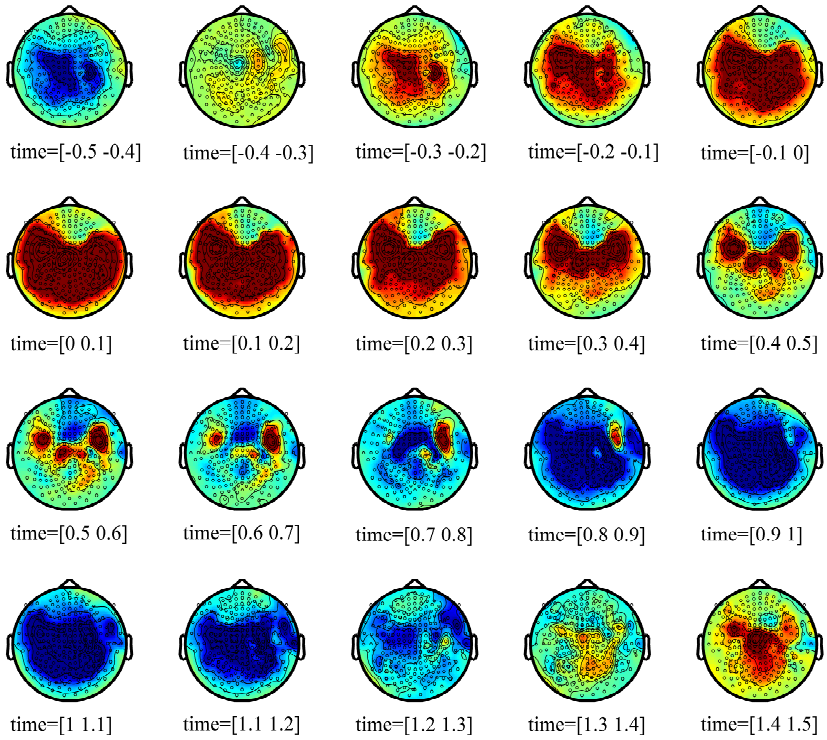

Figure 5.8: Topographical distribution over the head of beta activity (12-25 Hz) from -0.5-1.5 s for the even condition.

Chapter 6

Discussion and Analysis

6.1 Summary of Findings

The results presented in chapter 5 are summarised graphically in figure 6.1. This figure shows the relationship between ERFs (the blue and red traces) and induced potentials (time-frequency plots) for even and "no number" conditions over the left temporoparietal region. ERFs and TFRs are practically identical for even and odd conditions. Prior to the stimulus onset, a readiness field is observed in the ERF when a number is about to be displayed.

For the "no number" condition, beta-band desynchronisation and delta/theta-band synchronisation occurs from 0-0.7 s. The latter is indicative of a state of drowsiness and inattentiveness as the subject waits idly for the next trial. However, the former is probably indicative of subconscious categorical action planning in anticipation of the next trial. During this period, it is important to note that the N100, P200 and N200 ERF waveforms occur just after $t = 0\,s$. This series of events indicates that the brain is not completely idle, but carries out higher-order perceptual processing followed by the Go-NoGo control procedure which inhibits a motor response (button press).

For the even condition, event-related synchronisation in beta activity occurs throughout both hemispheres, but particularly so in the temporoparietal and frontal regions (not shown in figure 6.1). The topographical maps show an increased ERF amplitude near the left general interpretive area which is responsible for the execution of logical and mathematical operations. From 0-0.7 s, the subject is relaxed, focused, alert and actively concentrating

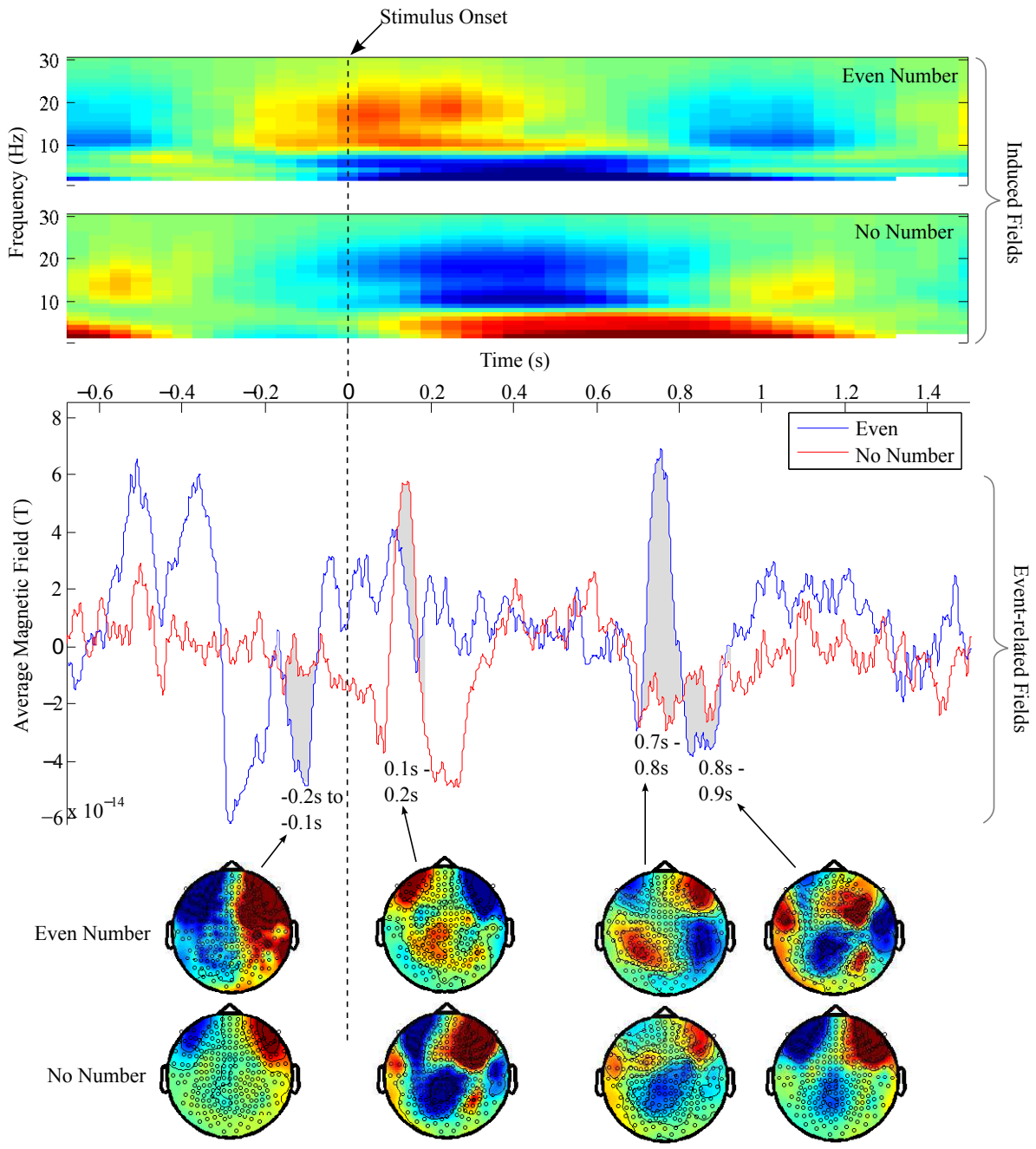

Figure 6.1: Diagram comparing ERFs, TFRs and topographical maps for even and no number conditions

on the mental task. It is important to note that the ERF waveform is nearly identical to that of the "no number" condition, but shifted in time by about $610\,ms$. One may therefore infer that the N100, P200 and N200 ERF waveforms occur later in time. This inference is confirmed by other research findings which showed that during arithmetic tasks, neural activity occurs in the frontal and pre-frontal regions with latencies of around $700-900ms$ [23].

The ERF waveform components are indicative of three sequential events in the brain: mental matching of the stimulus with previously experienced stimuli (N100), higher-order perceptual processing and comparison to stored memory (P200), and finally, the Go-NoGo control procedure which initiates the motor response (N200). During the mental calculation process, pronounced beta-band synchronisation occurs. As the motor action is subsequently carried out, one naturally observes desynchronisation within the beta band, and an ERF magnitude increase in the right frontal and pre-frontal regions. The entire mental calculation and response occurs within a period of $1\,s$ post-stimulus.

6.1.1 Parity and Memory

The complexities of the human brain are only vaguely understood, though many different models have sought to explain its behaviour. For example, some studies have proposed that numbers are represented as notation-independent forms in the memory [41]. Others suggest that arithmetic facts such as number magnitude and parity are stored in phonological form, semantic form or in multiple formats [42]. Overall, there is a consensus that neurons in the intraparietal sulcus (IPS) in the parietal lobe form a complex network that enables humans to attach arbitrary spoken or written symbols to an internal representation of the number stored in memory. This is evidenced by the fact that lesions in the IPS lead to impairments in basic numerical magnitude processing [43]. Furthermore, it is recognised that natural intelligence is memory-based [44].

It is no wonder, then, that evidence in this experiment points to the fact that memory plays an important role in the execution of the arithmetic task. The presence of the P200 wave is indicative of the use of stored memory. The author proposes that parity information is simply recalled from long-term memory - i.e., "*parity information is retrieved directly from memory rather than being extracted by means of a mental calculation strategy*" [45].

This would naturally be the case, since the mental calculation is simple and does not require complex cognition. Regardless of how large the number is, one can simply check the units digit to determine the parity of the entire number. The absence of gamma activity unilaterally and high beta activity in the parietal lobes is consistent with the view that mental parity selection does not require the use of higher mental processes.

The physiological foundation of long-term memory is the pre-motor cortex in the frontal lobe [46]. The supplementary and primary motor cortices are also involved in the regulation of "action buffer memory" which denotes memory functions for output-orientated actions [46]. In light of this, it is overly restrictive to limit the functional responsibilities of the motor cortices in the frontal lobe to only the coordination of movements. The induced and evoked fields present in the frontal lobe during the trial period (see figures 5.8 and 5.4a) may therefore be indicative of the use of memory as well as the coordination of the motor response.

6.1.2 Readiness Potential

One interesting finding is that a readiness potential (RP) - or in the context of MEG, a readiness field - is observed before the onset of the stimulus. Figure 6.1 shows the readiness field before $t = 0\,s$ in the "even" condition ERF. This is seen in the amplitude variations of the ERFs, the dispersion and subsequent polarity switch of the frontal dipole, and the increase in beta activity before $t = 0\,s$ (for the even and odd conditions). These observations indicate some sort of anticipatory response similar to the Bereitschaftspotential (or readiness potential) demonstrated by Libet *et al.* [47]. The readiness potential is traditionally a measure of activity leading up to voluntary muscle movement. More recently, fMRI and direct electrode recording have borne out the readiness potential experiments. Soon *et al.* [48] allowed subjects to decide to press either a left or right button whenever they felt the urge to do so. It was shown that there was spatially organised activity in the polar frontal cortex and parietal cortex that predicted the conscious left/right decision and preceded it by several seconds. Furthermore, one could even use fMRI to predict which button will be used well before any conscious decision is reported.

In this experiment, it is also possible to predict whether a number or no number is displayed by looking at the ERFs and TFRs before the stimulus onset. The reason for this is trivial. A small cross is displayed before a number, and is not displayed before no number. As the cross is displayed, the subject elicits a readiness field in anticipation of carrying out the task.

Section 5.3 shows that beta synchronisation occurs around the motor cortex (medially) and motor association area (laterally), followed by desynchronisation as the user presses the button. Activity in the motor association area prior to the motor action is indicative of a motor readiness field. This field is distinct from the pre-stimulus ERFs discussed above. The author proposes that the former is a readiness field associated with anticipation of carrying out the motor action (pressing the button), while the the latter is a readiness field associated with anticipation of carrying out the cognitive procedure (choosing between even or odd). Alternatively, one could argue that both readiness fields are associated with the motor action, since these fields may occur several seconds before the action is carried out [48].

6.1.3 Brain Lateralisation

It must be acknowledged that ERF or TFR topographical maps are only an estimate of the location of neuronal sources. Without proper source reconstruction, one cannot determine the exact location of neuronal sources with great accuracy. However, based on regional estimates, the results do confirm previous research findings regarding the functional regions of the brain. In particular, the ERF findings presented in section 5.2 confirm the well-established fact that the brain is lateralised according to function. This finding challenges the notion that brain lateralisation is not observed in MEG signals associated with mental arithmetic tasks [49]. Lateralisation refers to the functional specialisation of the brain in different hemispheres. While induced potentials are very similar in both hemispheres, ERFs are not; significant ERF variations are clearly observed in only one hemisphere. The results show that the left general interpretive area and right motor/premotor areas are involved in the calculative and motor aspects of the task. There are also anterior and posterior

differences that confirm other research findings [49] - activity associated with the computational task occurs mainly in the parietal lobes, whereas motor activity occurs in the frontal lobes.

Chapter 7

Conclusion

In this study, magnetoencephalography is used as a means of studying the spatial and temporal dynamics of the brain as subjects carry out a simple numerical task - choosing between an even or odd number. Data are recorded using a 248 channel MEG device. The data are first proprocessed using graphical methods and semi-automated methods like independent component analysis (ICA). The rest of the analysis involves finding, visualising and analysing evoked fields that are phase-locked to stimuli and background oscillatory rhythms that are not necessarily phase-locked to the stimuli. The evoked responses are found by averaging the MEG signals in selected brain regions over hundreds of trials. Induced responses are determined by averaging the time-frequency representations (TFRs) over trials. The TFRs were found using Wavelet analysis.

The N100, P200 and N200 event-related field (ERF) waveforms occur just after the onset of the stimulus. These waveforms indicate that the brain is involved in the following sequence of events: mental matching of the stimulus with previously experienced stimuli (N100), higher-order perceptual processing modulated by attention (P200), and "Go-NoGo" control procedure which initiates or inhibits the motor response (N200). The P200 response is also indicative of the use of stored memory, leading to the conclusion that parity information is retrieved directly from memory rather than being extracted by means of a mental calculation strategy. There is also clear evidence of a readiness field associated with the numerical task and motor action, as well as brain lateralisation. The research findings

confirm that the general interpretive area (Wernicke's area) in the left cerebral hemisphere is involved in the execution of simple mathematical tasks.

With regard to induced fields, the results show pronounced synchronisation in the beta-band close to the general interpretative area. During this period, the subject is relaxed, focused, alert and actively concentrating on the mental task. Thereafter, beta band desynchronisation occurs, as is normally the case when a motor response is carried out.

Recommendations

The field of computational neuroscience is vast, and there are many possible avenues of future work. The following recommendations are made for future work:

- Carry out source reconstruction using a technique such as beamforming. The MEG spatial estimation of primary neuronal currents (source estimates) is usually superimposed on top of an MRI of the subject or onto a normalised space such as Montreal Neurological Institute (MNI) standard brain [3]. Source reconstruction will enable one to identify functional regions of the brain more accurately than by simply using 2D topographical maps of ERFs/TFRs.

- Carry out a functional connectivity analysis which describes brain function in terms of the way information is transmitted and integrated across brain networks. Inferences about connectivity can be made from the correlations between source time-courses [50]. One study suggests that arithmetic processing depends on crosstalk between and within the parietal cortex and that this crosstalk contributes to one's numerical competence [51].

- Investigate whether there is coherence or phase synchronisation between frequency bands or between different functional regions. One study suggests that cross-spectral integration between neuronal oscillations in the gamma and alpha bands plays a completely distinct or even complementary roles in stimulus processing [52].

- Further investigate the relationship between evoked responses and induced rhythms. Some studies adduce reasons in support of an independent or additive model [53]

while others support a dependent model [2]. Some suggest that there is dependence via phase resetting and asymmetry of the rhythms [54].

- A promising direction for future research appears to be a combined use of fMRI and MEG performed separately on the same subject [10]. This would help to overcome the inverse problem which is significant in MEG due to the poorer spatial resolution.

References

[1] Henry Gray. *Anatomy of the human body*. Lea and Febiger, 1918.

[2] Hannu Laaksonen. *Cortical rhythms as markers of neural processing*. Doctoral thesis, Aalto University, O.V.Lounasmaa Laboratory, 2012.

[3] Peter Hansen, Morten Kringelbach, and Riitta Salmelin. *MEG: An Introduction to Methods*. Oxford University Press, USA, 1 edition, June 2010.

[4] Robert Oostenveld, Pascal Fries, Eric Maris, and Jan-Mathijs Schoffelen. FieldTrip: event related averaging and planar gradient. [Online]. Available: http://fieldtrip.fcdonders.nl/tutorial/timefrequencyanalysis. [Accessed: 28-Feb-2013].

[5] Stephen Whitmarsh. FieldTrip: Scripting. [Online]. Available: http://fieldtrip.fcdonders.nl/tutorial/scripting. [Accessed: 23-Aug-2013].

[6] Frederic H. Martini. *Fundamentals of Anatomy & Physiology, Sixth Edition*. Benjamin Cummings, 6 edition edition, January 2003.

[7] Todd C. Handy. *Event-related Potentials: A Methods Handbook*. MIT Press, 2005.

[8] Steven J Luck. *An introduction to the event-related potential technique*. The MIT Press, Cambridge (MA); London, 2005.

[9] Shravani Sur and V. K. Sinha. Event-related potential: An overview. *Industrial Psychiatry Journal*, 18(1):70–73, 2009. PMID: 21234168 PMCID: PMC3016705.

[10] P P Mitra and B Pesaran. Analysis of dynamic brain imaging data. *Biophysical journal*, 76(2):691–708, February 1999. PMID: 9929474.

[11] Hannu Laaksonen. *Cortical activity during speech and non-speech oromotor tasks: a magnetoencephalography (MEG) study*. Ph.D. dissertation, Aalto University, O.V.Lounasmaa Laboratory, October 2012. PMID: 22926020.

[12] Tallon-Baudry and Bertrand. Oscillatory gamma activity in humans and its role in object representation. *Trends in cognitive sciences*, 3(4):151–162, April 1999. PMID: 10322469.

[13] A. R Crossman and David Neary. *Neuroanatomy: an illustrated colour text*. Churchill Livingstone, Edinburgh; New York, 2010.

[14] Jaakko Malmivuo and Robert Plonsey. *Bioelectromagnetism: principles and applications of bioelectric and biomagnetic fields*. Oxford University Press, New York, 1995.

[15] Joseph D Bronzino. *Biomedical engineering fundamentals*. CRC/Taylor & Francis, Boca Raton, 2006.

[16] Carolin J Sheridan, Tamara Matuz, Rossitza Draganova, Hari Eswaran, and Hubert Preissl. Fetal magnetoencephalography - achievements and challenges in the study of prenatal and early postnatal brain responses: A review. *Infant and child development*, 19(1):80–93, 2010. PMID: 20209112.

[17] Teresa Montez, Simon-Shlomo Poil, Bethany F. Jones, Ilonka Manshanden, Jeroen P. A. Verbunt, Bob W. van Dijk, Arjen B. Brussaard, Arjen van Ooyen, Cornelis J. Stam, Philip Scheltens, and Klaus Linkenkaer-Hansen. Altered temporal correlations in parietal alpha and prefrontal theta oscillations in early-stage alzheimer disease. *Proceedings of the National Academy of Sciences*, 106(5):1614–1619, March 2009.

[18] Riitta Salmelin. Clinical neurophysiology of language: the MEG approach. *Clinical neurophysiology: official journal of the International Federation of Clinical Neurophysiology*, 118(2):237–254, February 2007. PMID: 17008126.

[19] Joachim Gross, Sylvain Baillet, Gareth R Barnes, Richard N Henson, Arjan Hillebrand, Ole Jensen, Karim Jerbi, Vladimir Litvak, Burkhard Maess, Robert Oostenveld, Lauri Parkkonen, Jason R Taylor, Virginie van Wassenhove, Michael Wibral, and Jan-Mathijs Schoffelen. Good practice for conducting and reporting MEG research. *NeuroImage*, 65:349–363, January 2013. PMID: 23046981.

[20] G Pfurtscheller and F H Lopes da Silva. Event-related EEG/MEG synchronization and desynchronization: basic principles. *Clinical neurophysiology: official journal of the International Federation of Clinical Neurophysiology*, 110(11):1842–1857, November 1999. PMID: 10576479.

[21] Frank Van Overwalle, Sofie Van den Eede, Kris Baetens, and Marie Vandekerckhove. Trait inferences in goal-directed behavior: ERP timing and localization under spontaneous and intentional processing. *Social cognitive and affective neuroscience*, 4(2):177–190, June 2009. PMID: 19270041.

[22] C Miniussi, C A Marzi, and A C Nobre. Modulation of brain activity by selective task sets observed using event-related potentials. *Neuropsychologia*, 43(10):1514–1528, 2005. PMID: 15989941.

[23] Hiroko Kou and Sunao Iwaki. Modulation of neural activities by the complexity of mental arithmetic: An MEG study. *International Congress Series*, 1300:539–542, June 2007.

[24] H R Dinse, K Krüger, A C Akhavan, F Spengler, G Schöner, and C E Schreiner. Low-frequency oscillations of visual, auditory and somatosensory cortical neurons evoked by sensory stimulation. *International journal of psychophysiology: official journal of the International Organization of Psychophysiology*, 26(1-3):205–227, June 1997. PMID: 9203004.

[25] Scott Makeig and Tzyy-Ping Jung. Tonic, phasic, and transient EEG correlates of auditory awareness in drowsiness. *Cognitive Brain Research*, 4(1):15–25, July 1996.

[26] R Hari and R Salmelin. Human cortical oscillations: a neuromagnetic view through the skull. *Trends in neurosciences*, 20(1):44–49, January 1997. PMID: 9004419.

[27] Fabian J Theis and Anke Meyer-Bäse. *Biomedical signal analysis: contemporary methods and applications*. MIT Press, Cambridge, MA, 2010.

[28] John L Semmlow. *Biosignal and biomedical image processing: MATLAB-based applications*. CRC ; Taylor & Francis [distributor], Boca Raton, Fla.; London, 2008.

[29] Anthony J. Bell and Terrence J. Sejnowski. An information-maximization approach to blind separation and blind deconvolution. *Neural computation*, 7(6):1129–1159, 1995.

[30] Andreas Bruns. Fourier-, hilbert- and wavelet-based signal analysis: are they really different approaches? *Journal of neuroscience methods*, 137(2):321–332, August 2004. PMID: 15262077.

[31] Yuval Harpaz. Bar Ilan University MEG GitHub Repository. [Online]. Available: https://github.com/yuval-harpaz. [Accessed: 28-Feb-2013].

[32] Stephen Whitmarsh. FieldTrip: Walkthrough. [Online]. Available: http://fieldtrip.fcdonders.nl/walkthrough. [Accessed: 21-Jun-2013].

[33] Kristina M. Ropella. *Introduction to Statistics for Biomedical Engineers*. Morgan and Claypool Publishers, Marquette University, 2007.

[34] John H. McDonald and University of Delaware. *Handbook of Biological Statistics*. Sparky House Publishing, 2009.

[35] Robert Oostenveld, Pascal Fries, Eric Maris, and Jan-Mathijs Schoffelen. FieldTrip: time-frequency analysis using hanning window, multitapers and wavelets. [Online]. Available: http://fieldtrip.fcdonders.nl/tutorial/timefrequencyanalysis. [Accessed: 28-Feb-2013].

[36] Hang Su and Jingsong Li. Adaptive approach based on curve fitting and interpolation for boundary effects reduction. *WSEAS Transaction on Signal Processing*, 9(1), January 2013.

[37] Jonathan R Folstein and Cyma Van Petten. Influence of cognitive control and mismatch on the n2 component of the ERP: a review. *Psychophysiology*, 45(1):152–170, January 2008. PMID: 17850238.

[38] Edward W. P. Schafer and Marilyn M. Marcus. Self-stimulation alters human sensory brain responses. *Science*, 181(4095):175–177, July 1973. PMID: 4711735.

[39] R Freunberger, W Klimesch, M Doppelmayr, and Y Höller. Visual p2 component is related to theta phase-locking. *Neuroscience letters*, 426(3):181–186, October 2007. PMID: 17904744.

[40] Hame Park, June Sic Kim, and Chun Kee Chung. Differential beta-band event-related desynchronization during categorical action sequence planning. *PLoS ONE*, 8(3):e59544, March 2013.

[41] Roi Cohen Kadosh and Vincent Walsh. Numerical representation in the parietal lobes: abstract or not abstract? *The Behavioral and brain sciences*, 32(3-4):313–328; discussion 328–373, August 2009. PMID: 19712504.

[42] T Harmony, T Fernández, J Silva, J Bosch, P Valdés, A Fernández-Bouzas, L Galán, E Aubert, and D Rodríguez. Do specific EEG frequencies indicate different processes during mental calculation? *Neuroscience letters*, 266(1):25–28, April 1999. PMID: 10336175.

[43] Daniel Ansari and Annette Karmiloff-Smith. Atypical trajectories of number development: a neuroconstructivist perspective. *Trends in cognitive sciences*, 6(12):511–516, December 2002. PMID: 12475711.

[44] Yingxu Wang and Ying Wang. Cognitive models of the brain. In *First IEEE International Conference on Cognitive Informatics, 2002. Proceedings*, pages 259–269, 2002.

[45] D B Berch, E J Foley, R J Hill, and P M Ryan. Extracting parity and magnitude from arabic numerals: developmental changes in number processing and mental representation. *Journal of experimental child psychology*, 74(4):286–308, December 1999. PMID: 10552920.

[46] S. Marc Breedlove, Neil V Watson, and Mark R Rosenzweig. *Biological psychology: an introduction to behavioral, cognitive, and clinical neuroscience*. Sinauer Associates, Inc. Publishers, Sunderland, MA, 6 edition, 2010.

[47] B Libet, C A Gleason, E W Wright, and D K Pearl. Time of conscious intention to act in relation to onset of cerebral activity (readiness-potential). the unconscious initiation of a freely voluntary act. *Brain: a journal of neurology*, 106 (Pt 3):623–642, September 1983. PMID: 6640273.

[48] Chun Siong Soon, Marcel Brass, Hans-Jochen Heinze, and John-Dylan Haynes. Unconscious determinants of free decisions in the human brain. *Nature Neuroscience*, 11(5):543–545, May 2008.

[49] J Fell, J Röschke, M Grözinger, H Hinrichs, and H Heinze. Alterations of continuous MEG measures during mental activities. *Neuropsychobiology*, 42(2):99–106, 2000. PMID: 10940765.

[50] J.P. Owen, D.P. Wipf, H.T. Attias, K. Sekihara, and S.S. Nagarajan. Robust methods for reconstructing brain activity and functional connectivity between brain sourceswith meg/eeg data. In *Biomedical Imaging: From Nano to Macro, 2009. ISBI '09. IEEE International Symposium on*, pages 1271–1274, 2009.

[51] Joonkoo Park, Denise C Park, and Thad A Polk. Parietal functional connectivity in numerical cognition. *Cerebral cortex (New York, N.Y.: 1991)*, July 2012. PMID: 22784605.

[52] Satu Palva. *Neuronal Oscillations in Gamma- and Alpha-frequency Bands: From Object Representations to Sensory Awareness*. PhD thesis, University of Helsinki, 2007.

[53] Ankoor S. Shah, Steven L. Bressler, Kevin H. Knuth, Mingzhou Ding, Ashesh D. Mehta, Istvan Ulbert, and Charles E. Schroeder. Neural dynamics and the fundamental mechanisms of event-related brain potentials. *Cerebral Cortex*, 14(5):476–483, 2004.

[54] S. Makeig, M. Westerfield, T.-P. Jung, S. Enghoff, J. Townsend, E. Courchesne, and T. J. Sejnowski. Dynamic brain sources of visual evoked responses. *Science*, 295(5555):690–694, January 2002. PMID: 11809976.

Appendix A

Contaminated Trials and Channels

Tables A.1-A.4 show the trials and channels contaminated by artifacts, and the total number of remaining trials after elimination through visual inspection.

Table A.1: Trials/channels removed through visual artifact rejection (subject 1).

	Trials Removed	Channels Removed	Number of Remaining Trials
Even	10, 11, 35	A204, A74, 175, 176, 113, 153	106
Odd	8, 16, 29, 30, 32, 57, 91	A204, A74, 153, 176	84
No Num	13, 15, 23, 32, 120, 158, 167, 200	A204, A74, 153, 176	193

Table A.2: Trials/channels removed through visual artifact rejection (subject 2).

	Trials Removed	Channels Removed	Number of Remaining Trials
Even	12, 13, 54, 57, 58, 63, 80, 100	A204, A74, A228, A194, A193, A227, A195	97
Odd	7, 20, 22, 76, 77	A204, A74, A228, A194, A193, A227, A195	90
No Num	11, 15, 57, 90, 106, 117, 155, 156, 190	A204, A74, A228, A194, A195	191

Table A.3: Trials/channels removed through visual artifact rejection (subject 3).

	Trials Removed	Channels Removed	Number of Remaining Trials
Even	3, 4, 5, 6, 7, 58, 68, 85	A204, A74, A228, A194, A227, A195	103
Odd	4, 6, 7, 16, 17, 32, 68, 69, 72	A204, A74, A228, A247, A194, A227, A195	80
No Num	1, 47, 78, 87, 101, 120, 144, 153, 154, 155, 157	A204, A74	191

Table A.4: Trials/channels removed through visual artifact rejection (subject 4).

	Trials Removed	Channels Removed	Number of Remaining Trials
Even	87, 92, 94, 100, 108	A204, A74	107
Odd	23, 47, 68, 76, 77, 84	A204, A74	82
No Num	58, 64, 65, 88, 121, 133, 147, 163, 175, 176, 191, 195	A204, A74, A114, A32	190

Appendix B

Statistical Parameters

Figures B.1 and B.2 show examples of noise caused by movement of the subject and electronic SQUID jumps.

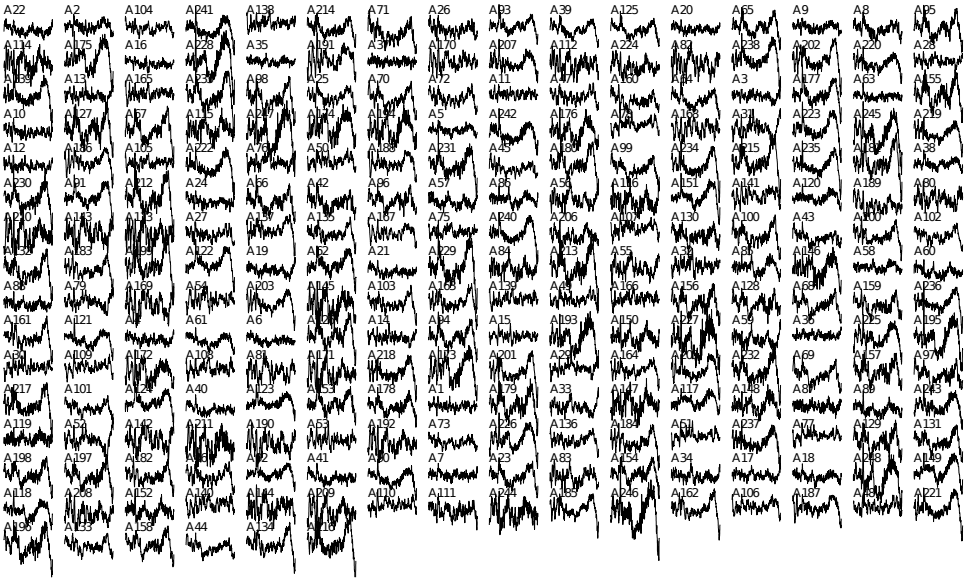

Figure B.1: Data segment for all channels showing movement artifacts. Note the negative D.C. shift across a large number of channels.

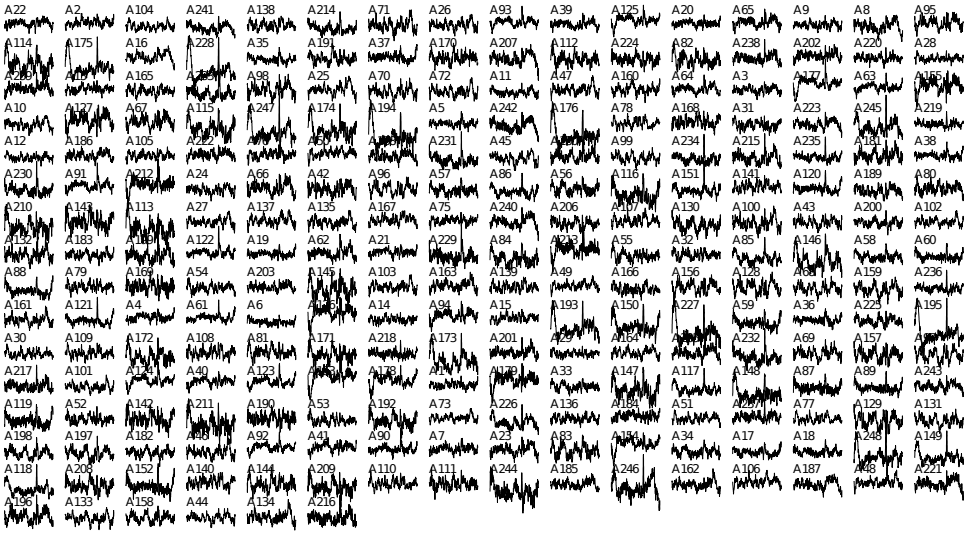

Figure B.2: Data segment for all channels showing SQUID jumps. Note the sharp positive spike present across a large number of channels.

Appendix C

MATLAB Code

The MATLAB code used in preprocessing and analysing the data is presented in this appendix. Listing C.1 contains the script used to preprocess and analyse the MEG data using parallel processing in MATLAB. Listing C.2 contains a separate script used for removing visual artifacts and for visualising ICA results. An example of how to implement Bar-Ilan's cleaning script is shown in Listing C.3. Lastly, Listings C.4 and C.5 show the code used in calculating grand averages for all subjects and plotting the averaged evoked and induced potentials.

Listing C.1: Code used to preprocess and analyse the MEG data using MATLAB's Parallel toolbox.

```
1  % ----------------------------------------
2  %
3  % MEG Analysis Protocol: Even and Odd Numbers
4  %
5  % Author: Graham Peyton
6  % Markers:
7  %     TRIGGERS: 40 (even), 50 (odd), 2048 (nothing happens)
8  %     RESPONSES: 256 (even), 512 (odd)
9  %
10 % Notes:
11 %   The numbers were displayed for as long as needed (until button
       press).
12 %   There was 1 second break between a press and the next number
       screening.
13 %
```

```
14 % ------------------------------------------
15
16 % addpath(genpath('/Users/Graham/Documents/MEG analysis/cleanMEG_BIU
       '));
17 addpath(genpath('/Users/Graham/Documents/MEG analysis/FieldTrip'));
18
19 % Prepare the parallel Processing
20 matlabpool open local 3 % Quad core
21
22 % These path are to data processed with the Bar-Ilan script
23 subjectlist = {
24     % Subject A
25     '/Users/Graham/Documents/MEG analysis/odd08_2/,14d2/16.11.10
          @_10_57/1/xc,lf_c1,rfhp0.1Hz'
26     % Subject B
27     '/Users/Graham/Documents/MEG analysis/odd06/,14d2n/10.11.10
          @_10_24/1/xc,hb,lf_c,rfhp0.1Hz'
28     % Subject C
29     '/Users/Graham/Documents/MEG analysis/odd04/oddDi/15.02.10@09_21
          /1/hb,lf_c1,rfhp0.1Hz'
30     % Subject D
31     '/Users/Graham/Documents/MEG analysis/odd03/oddDi/09.02.10@09_58
          /1/lf_c,rfhp0.1Hz'
32 };
33
34 conditionlist = {
35   'even'
36   'odd'
37   'noNum'
38 };
39
40 triggercode = [
41   40
42   50
43   2048
44 ];
45
46 % Definition of all the noisy trials and channels for all subjects.
47 % Note that the repeated 0s or '-A204's are simply to make the size
       nxm
48 %% Odd08_2
49 noisyTrialsA = [
50     [10, 11, 35, 10, 10, 10, 10, 10]                    % Variance
          3.2e-25
51     [8, 16, 29, 30, 32, 57, 91, 8]                      % Variance
          0.29e-24
52     [13, 15, 23, 32, 120, 158, 167, 200]                % Variance
          2.5e-25
```

```
];
channelsA = {
    {'MEG','-A204','-A74', '-A175', '-A176', '-A113', '-A153'}
    {'MEG','-A204','-A74', '-A176', '-A153', '-A204', '-A204'}
    {'MEG','-A204','-A74', '-A176', '-A153', '-A204', '-A204'}
};
%% Odd06
noisyTrialsB = [
    [12, 13, 54, 57, 58, 63, 80, 100, 12]       % Variance 0.5e-24
    [7, 20, 22, 76, 77, 7, 7, 7, 7]             % Variance 0.5e-24
    [11, 15, 57, 90, 106, 117, 155, 156, 190]   % Variance 0.5e-24
];
channelsB = {
    {'MEG','-A204','-A74', '-A227', '-A228', '-A193', '-A194', '-
        A195'}
    {'MEG','-A204','-A74', '-A227', '-A228', '-A193', '-A194', '-
        A195'}
    {'MEG','-A204','-A74', '-A194', '-A195', '-A204', '-A204', '-
        A204'}
};

%% Odd04
noisyTrialsC = [
    [3, 4, 5, 6, 7, 58, 68, 85, 3, 3, 3]                % Variance
        3.2e-25
    [4, 6, 7, 16, 17, 32, 68, 69, 72, 4, 4]             % Variance
        0.29e-24
    [1, 47, 78, 87, 101, 120, 144, 153, 154, 155, 157]  % Variance
        2.5e-25
];
channelsC = {
    {'MEG','-A204','-A74', '-A228', '-A194', '-A227', '-A195', '-
        A204'}
    {'MEG','-A204','-A74', '-A228', '-A247', '-A194', '-A227', '-
        A195'}
    {'MEG','-A204','-A74', '-A204', '-A204', '-A204', '-A204', '-
        A204'}
};
%% Odd03
noisyTrialsD = [
    [87, 92, 94, 100, 108, 87, 87, 87, 87, 87, 87, 87]
        % Variance 5e-25
    [23, 47, 68, 76, 77, 84, 23, 23, 23, 23, 23, 23]
    [58, 64, 65, 88, 121, 133, 147, 163, 175, 176, 191, 195]
];
channelsD = {
    {'MEG','-A204','-A74', '-A204', '-A204'}
    {'MEG','-A204','-A74', '-A204', '-A204'}
```

```
91      {'MEG','-A204','-A74', '-A32', '-A14'}
92  };
93  %% Group all the channels and noisy trials
94  noisyTrials = { noisyTrialsA noisyTrialsB noisyTrialsC noisyTrialsD
        };
95  channels = { channelsA channelsB channelsC channelsD };
96
97  % start with a new and empty configuration
98  % cfg1 = {};
99  avg = {};
100
101 %% Main computation loop
102 for subj=1:length(subjectlist)
103   parfor cond=1:length(conditionlist)
104     %% Preprocessing
105     cfg                       = [];
106     cfg.dataset               = subjectlist{subj};
107     cfg.trialdef.eventtype    = 'TRIGGER';
108     cfg.trialdef.eventvalue   = triggercode(cond);          % Even
109     cfg.trialdef.prestim      = 2.5;
110     cfg.trialdef.offset       = -2.5;
111     cfg.trialdef.poststim     = 2.5;
112     cfg.trialdef.powerline    = 'yes'; % takes into account triggers
            that contain the electricity in the wall (+256).
113     cfg.trialfun              ='BIUtrialfun';
114
115     cfg1                      = ft_definetrial(cfg);
116     cfg1.blc                  = 'yes';
117     cfg1.continuous           = 'yes';        % Interpret the data as
            continuous (this is before segmenting)
118     badTrials                 = noisyTrials{subj}(cond,:);
119     cfg1.trl(noisyTrials{subj}(cond,:),:) = [];
120     cfg1.channel              = channels{subj}{cond};
121     cfg1.bpfilter             = 'yes';
122     cfg1.bpfreq               = [1 100];      % Default fourth order
123     cfg1.baselinewindow       = [-0.5 -0.1];
124     cfg1.demean               = 'yes';
125     cfg1.dftfilter            = 'yes';        % line noise removal
            using discrete fourier transform
126     cfg1.dftfreq              = [24 50 100];  % Aircon and mains
127
128     data                      = ft_preprocessing(cfg1);
129
130     %% Time-locked analysis
131     cfg                       = [];
132     avg{cond}                 = ft_timelockanalysis(cfg,data);
133
134 %     %% Time-Frequency Analysis (Multitapers)
```

```
135 %     cfg = [];
136 %     cfg.output     = 'pow';
137 %     cfg.channel    = 'MEG';
138 %     cfg.method     = 'mtmconvol';
139 %     cfg.foi        = 1:2:30;           % Frequencies of interest
140 %     cfg.t_ftimwin  = 5./cfg.foi;        % Length of sliding window
      (5 cycles per time window)
141 %     cfg.tapsmofrq  = 0.4*cfg.foi;
142 %     cfg.toi        = -0.5:0.05:1.5;       % Time interval of
    interest (50ms)
143 %     cfg.pad        = 'maxperlen';
144 %     TFRmult{cond} = ft_freqanalysis(cfg, data);
145
146     %% Time-Frequency Analysis (Wavelets)
147     cfg = [];
148     cfg.channel    = 'MEG';
149     cfg.method     = 'wavelet';
150     cfg.width      = 5;
151     cfg.output     = 'pow';
152     cfg.foi        = 1:1:30;
153     cfg.toi        = -1.5:0.05:1.5;
154     TFRwave{cond} = ft_freqanalysis(cfg, data);
155
156   end
157   Average{subj} = avg;
158 %   AllTFRmult{subj} = TFRmult;
159   AllTFRwave{subj} = TFRwave;
160 end
161 % save('/Users/Graham/Documents/MEG analysis/Variables/0-30Hz_2/
      AllTFRmult.mat');
162 save('/Users/Graham/Documents/MEG analysis/Variables/0-30Hz_3/
      AllTFRwave.mat');
163 save('/Users/Graham/Documents/MEG analysis/Variables/0-30Hz_3/
      Average.mat');
164
165 matlabpool close
```

Listing C.2: Script used for visual artifact removal and Independent Components Analysis (ICA)

```
1 % ------------------------------------------
2 %
3 % MEG Analysis Protocol for rejecting visual artifacts
4 %
5 % Author: Graham Peyton
6 % Markers:
```

```
%     TRIGGERS: 40 (even), 50 (odd), 2048 (nothing happens)
%     RESPONSES: 256 (even), 512 (odd)
%
% ----------------------------------------

addpath(genpath('/Users/Graham/Documents/MEG analysis/FieldTrip'));

subjectlist = {
  '/Users/Graham/Documents/MEG analysis/odd03/oddDi/09.02.10@09_58
     /1/lf_c,rfhp0.1Hz'
};

cfg = {};

prestim     = 0.3;
poststim    = 1;
offset      = -0.3;

for subj=1:length(subjectlist)
    cfg                       = [];
    cfg.dataset               = subjectlist{subj};
    cfg.trialdef.eventtype    = 'TRIGGER';
    cfg.trialdef.eventvalue   = [2048]; % All conditions together
    cfg.trialdef.prestim      = prestim;
    cfg.trialdef.offset       = offset;
    cfg.trialdef.poststim     = poststim;
    cfg.trialdef.powerline    = 'yes';        % takes into account
       triggers that contain the electricity in the wall (+256).
    cfg.trialfun              = 'BIUtrialfun';

    cfg1                      = ft_definetrial(cfg);
    cfg1.blc                  = 'yes';
    cfg1.continuous           = 'yes';        % Interpret the data as
       continuous (this is before segmenting)
    cfg1.channel              = {'MEG','-A204','-A74'};
    cfg1.bpfilter             = 'yes';
    cfg1.bpfreq               = [1 100];      % Default fourth order

    cfg1.baselinewindow       = [-0.5 -0.1];
    cfg1.demean               = 'yes';
    cfg1.dftfilter            = 'yes';        % line noise removal
       using discrete fourier transform
    cfg1.dftfreq              = [24 50 100];  % Aircon and mains
    data                      = ft_preprocessing(cfg1); % reading the
       data

    %% Visual Artifact Rejection
    cfg           = [];
```

```
50      cfg.method    = 'trial';
51      cfg.alim      = 1e-12;
52      dummy         = ft_rejectvisual(cfg,data);
53      cfg.method    = 'summary';
54      cfg.alim      = 1e-12;
55      cfg.megscale  = 1;
56      dummy         = ft_rejectvisual(cfg,data);
57
58  %     % Independant Component Analysis Visualisation (uncomment if
        necessary)
59  %     cfg              = [];
60  %     cfg.resamplefs = 300;
61  %     cfg.detrend    = 'no';
62  %     dummy              = ft_resampledata(cfg, data);
63  %
64  %     cfg              = [];
65  %     cfg.channel      = 'MEG';
66  %     ic_data          = ft_componentanalysis(cfg,dummy);
67  %     cfg              = [];
68  %     cfg.channel      = [1:10]; % components to be plotted
69  %     cfg.layout       = '4D248.lay'; % specify the layout file that
        should be used for plotting
70  %     figure();
71  %     ft_databrowser(cfg, ic_data)
72
73  end
```

Listing C.3: Implementation of Bar-Ilan's MEG cleaning script.

```
1  % An example of how to use Bar Ilan's cleaning script
2  addpath(genpath('/Users/Graham/Documents/MEG analysis/cleanMEG_BIU')
       );
3  cd '/Users/Graham/Documents/MEG analysis/odd03/oddDi/09.02.10@09_58
       /1';
4
5  fileName = 'c,rfhp0.1Hz';
6
7  p=pdf4D(fileName);
8  cleanCoefs = createCleanFile(p, fileName,...
9       'byLF',256 ,'Method','Adaptive',...
10      'xClean',[4,5,6],...
11      'chans2ignore',[74,204],...
12      'byFFT',0,...
13      'HeartBeat',[],... % use [] for automatic HB cleaning, use 0 to
           avoid HB cleaning
14      'maskTrigBits', 512);
15
```

```
cd '/Users/Graham/Documents/Dropbox/Grahams Stuff/PostGrad/MEG Code'
```

Listing C.4: Code used for calculating the grand average of evoked potentials.

```
set(0,'DefaultAxesFontName', 'Times New Roman')
set(0,'DefaultAxesFontSize', 12)
set(0,'DefaultTextFontname', 'Times New Roman')
set(0,'DefaultTextFontSize', 12)

% Left frontal
cfgLF.channel = {'A40', 'A41', 'A64', 'A65', 'A66', 'A92', 'A93', '
    A94', 'A95', 'A124', 'A125', 'A126', 'A127', 'A128', 'A153', '
    A154', 'A155', 'A156', 'A177', 'A178', 'A179', 'A196', 'A212', '
    A213', 'A229', 'A230'}
% Right frontal
cfgRF.channel = {'A35', 'A36', 'A58', 'A59', 'A60', 'A85', 'A86', '
    A87', 'A88', 'A115', 'A116', 'A117', 'A118', 'A119', 'A147', '
    A148', 'A149', 'A150', 'A174', 'A175', 'A176', 'A193', 'A194', '
    A195'}
% Left parietal
cfgLP.channel = {'A11', 'A26', 'A27', 'A45', 'A46', 'A47', 'A48', '
    A70', 'A71', 'A72', 'A73', 'A74', 'A99', 'A100', 'A101', 'A102',
    'A103', 'A131', 'A132', 'A133', 'A134', 'A159', 'A160', 'A161', '
    A182'}
%Right parietal
cfgRP.channel = {'A29', 'A51', 'A52', 'A76', 'A77', 'A78', 'A79', '
    A106', 'A107', 'A108', 'A109', 'A110', 'A140', 'A141', 'A142', '
    A143', 'A168', 'A169', 'A170', 'A190', 'A191', 'A208'}

figure; hold on;
subplot(2,2,1); ft_singleplotER(cfgLF, grandEven, grandOdd,
    grandNoNum);
ylabel('Average Magnetic Field (T)'); xlabel('Time (s)'); title('
    Left Frontal')
xlim([-0.68 1.5])
subplot(2,2,2); ft_singleplotER(cfgRF, grandEven, grandOdd,
    grandNoNum);
%l = legend({'Even', 'Odd', 'No Number'},'Location','Best'); set(l,'
    FontSize',14);
ylabel('Average Magnetic Field (T)'); xlabel('Time (s)'); title('
    Right Frontal')
xlim([-0.68 1.5])
subplot(2,2,3); ft_singleplotER(cfgLP, grandEven, grandOdd,
    grandNoNum);
%l = legend({'Even', 'Odd', 'No Number'},'Location','Best'); set(l,'
    FontSize',14);
```

```
ylabel('Average Magnetic Field (T)'); xlabel('Time (s)'); title('
    Left Parietal')
xlim([-0.68 1.5])
subplot(2,2,4); ft_singleplotER(cfgRP, grandEven, grandOdd,
    grandNoNum);
%l = legend({'Even', 'Odd', 'No Number'},'Location','Best'); set(l,'
    FontSize',14);
ylabel('Average Magnetic Field (T)'); xlabel('Time (s)'); title('
    Right Parietal')
xlim([-0.68 1.5])
legend({'Even', 'Odd', 'No Number'},'Location','Best'); set(l,'
    FontSize',14);
```

Listing C.5: Code used for calculating the grand average of induced potentials.

```
addpath(genpath('/Users/Graham/Documents/MEG analysis/FieldTrip'));
% Change default axes and text fonts.
set(0,'DefaultAxesFontName', 'Times New Roman')
set(0,'DefaultAxesFontSize', 14)
set(0,'DefaultTextFontname', 'Times New Roman')
set(0,'DefaultTextFontSize', 14)

cfg = [];
cfg.baseline     = [-0.5 -0.1];
cfg.baselinetype = 'absolute';
cfg.zlim         = [-3e-24 3e-24];
% cfg.showlabels   = 'yes';
cfg.layout       = '4D248.lay';
cfg.interactive  ='yes';
cfg.fontsize     = 12;
figure
ft_multiplotTFR(cfg, grandEven)
```